

https://dspace.org/

Modelling the performance of Manganese electrowinning cells

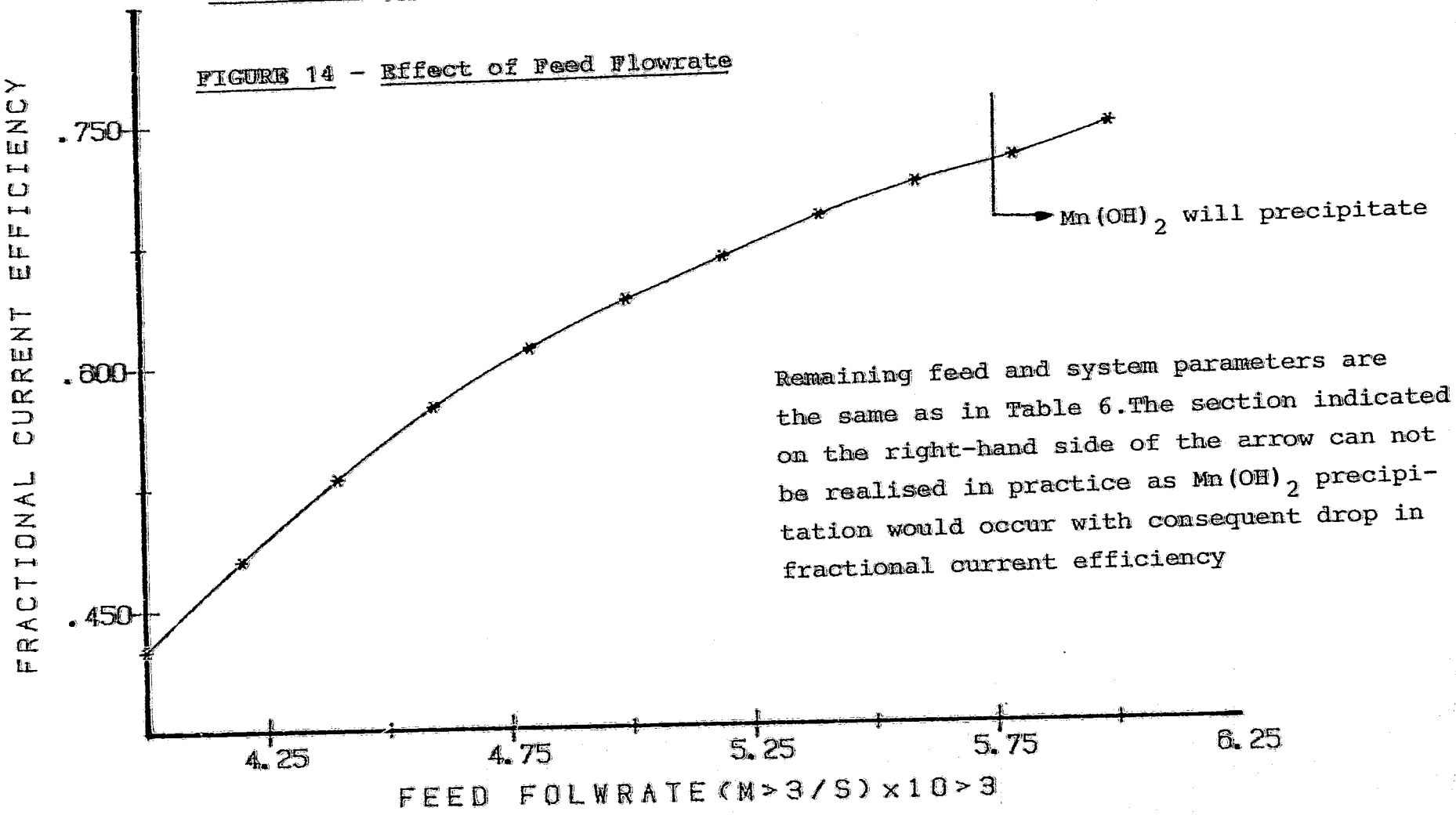
Rodrigues, Jose Carlos Pereira

2015
http://hdl.handle.net/10539/19221

Downloaded from a DSpace repository. https://dspace.org/

FRACTIONAL CURRENT EFFICIENCY VS FEED FLOWRATE

FIGURE 14 - Effect of Feed Flowrate



Remaining feed and system parameters are the same as in Table 6.The section indicated on the right-hand side of the arrow can not be realised in practice as $Mn(OH)_2$ precipitation would occur with consequent drop in fractional current efficiency

3.2.2 - Influence of pH on Fractional Current Efficiency

Figure 15 Shows the effect of changing the catholyte pH on fractional current efficiency.As expected,the current efficiency increases with pH up to a point where manganese hydroxide $Mn(OH)_2$ precipitates.When this condition occurs it is not practical to increase the pH any further as the overall plant performance will decrease drastically.

Figure 16 shows the results as published by MINTEK (6). The lower experimental current efficiencies were previously explained as being due to the way in which the MINTEK operations were performed.Higher current efficiencies are in fact found on industrial plants with a similar trend to that predicted.

TABLE 8 - Fractional Current Efficiency versus Catholyte pH

Fractional Current Efficiency	Catholyte pH
0,617	7,2
0,666	7,4
0,685	7,5
0,702	7,6
0,718	7,7
0,731	7,8
0,752	8,0

FIGURE 15 - FRACTIONAL CURRENT EFFICIENCY VS CATHOLYTE PH

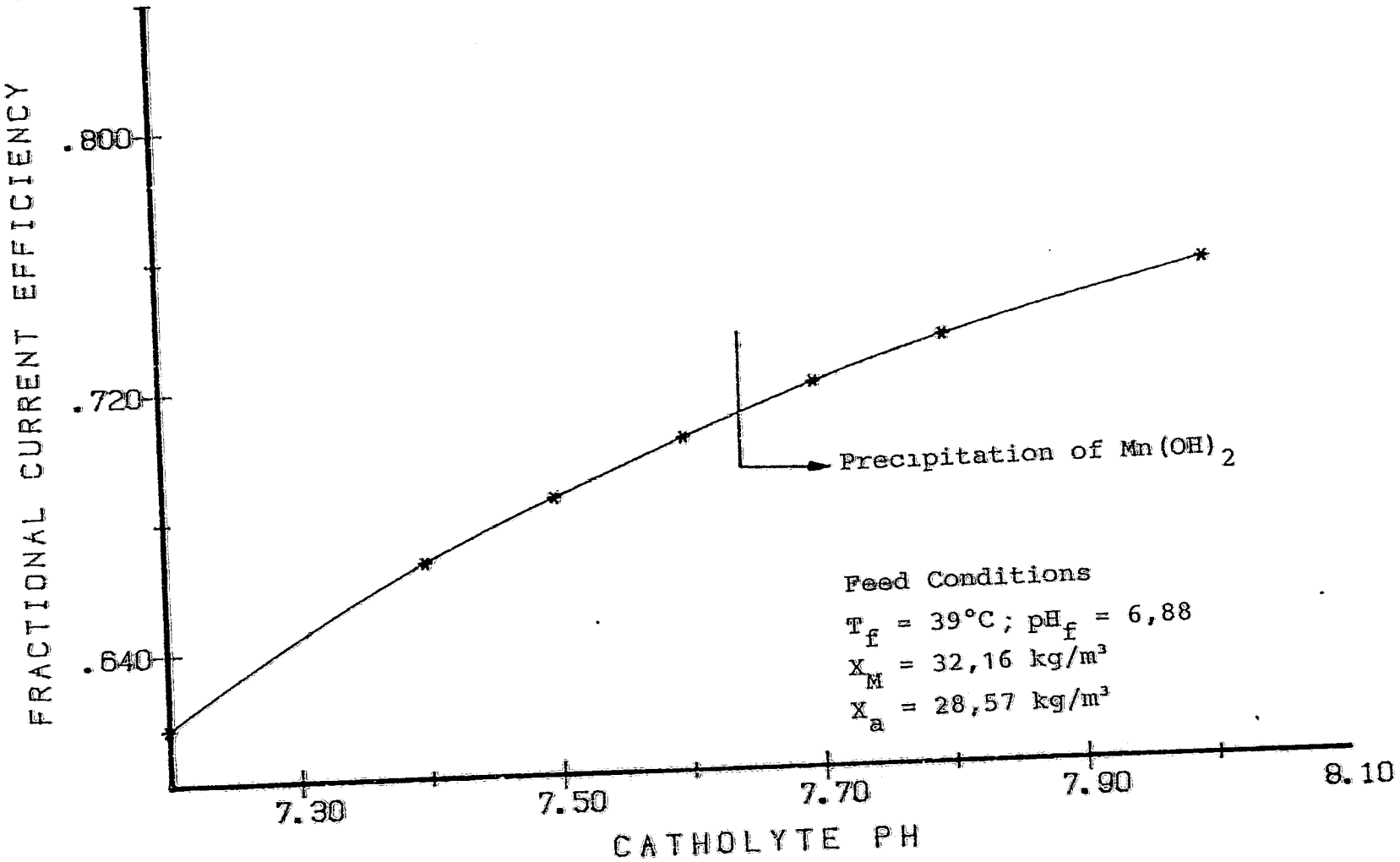


FIGURE 16 - Influence of pH on Current Efficiency as published by MINTEK (6)

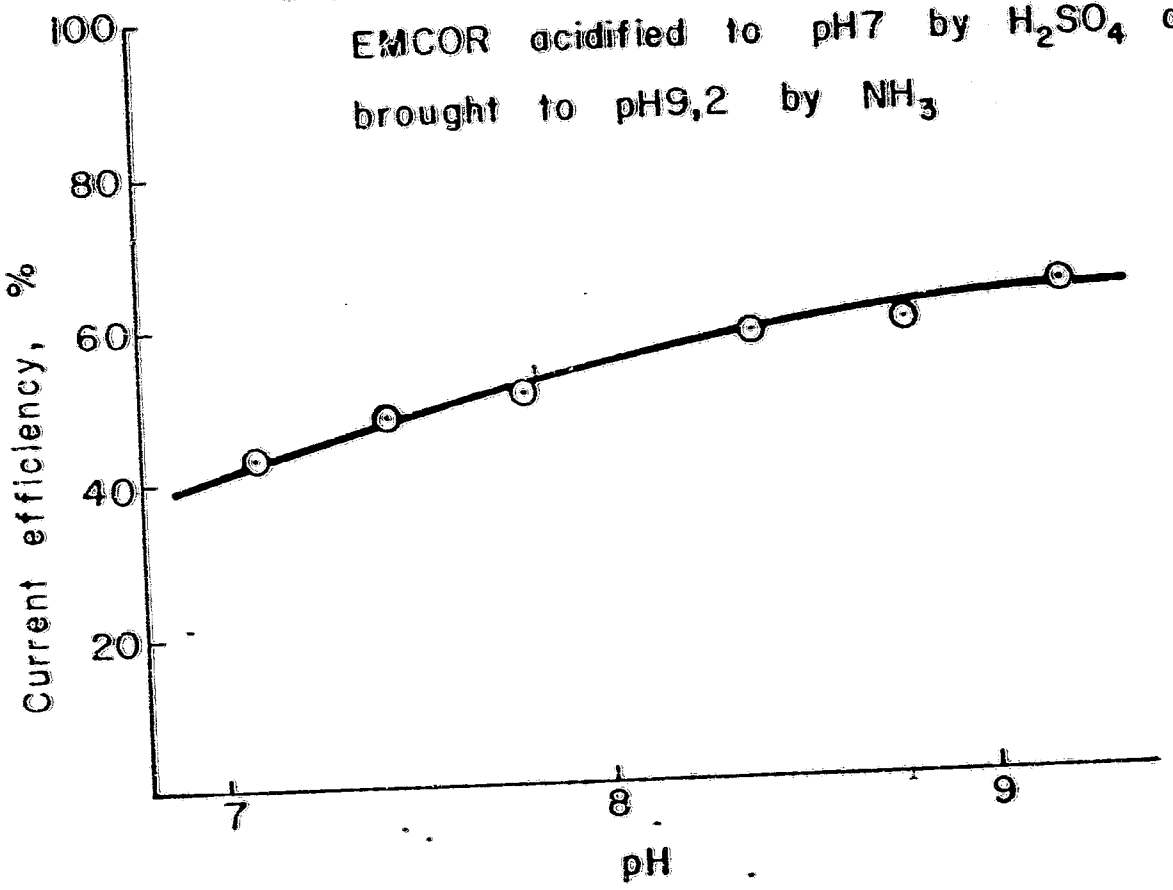
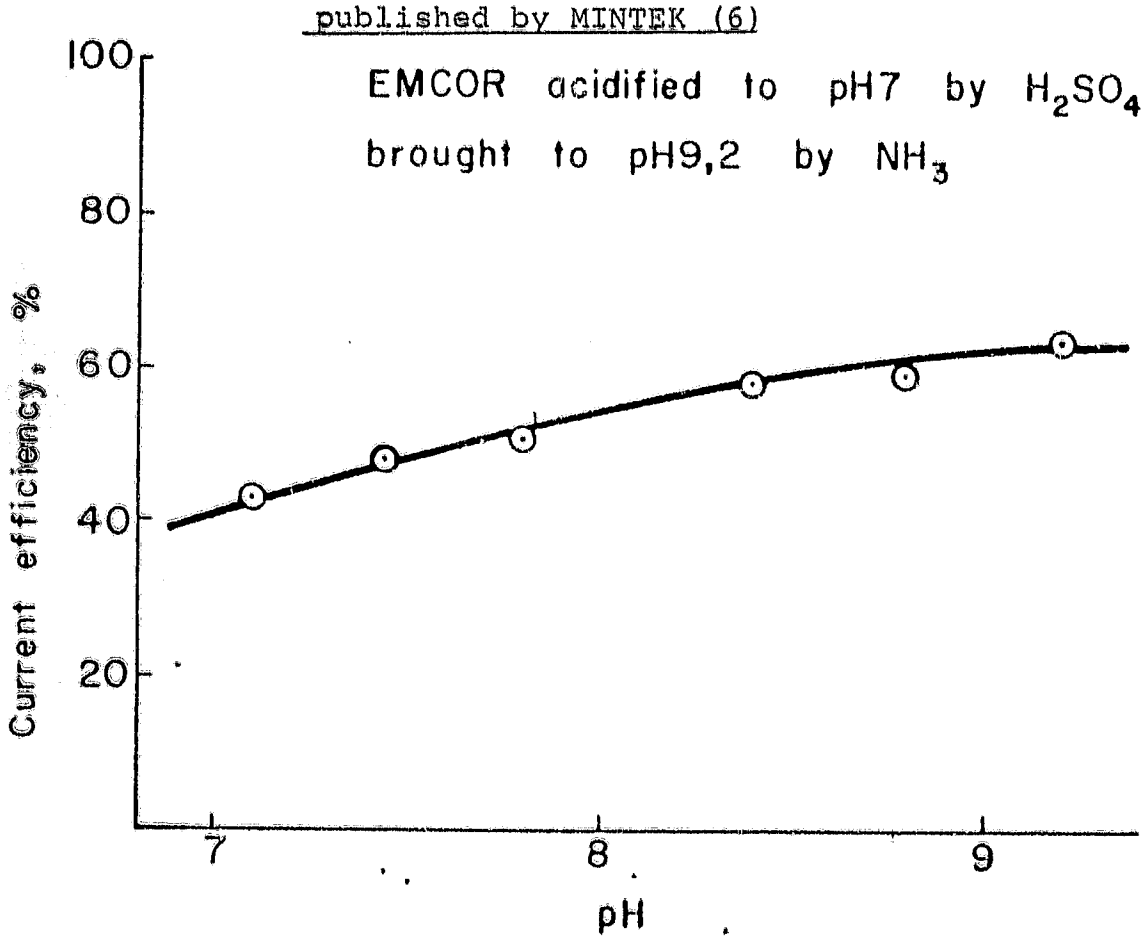


FIGURE 16 - Influence of pH on Current Efficiency as published by MINTEK (6)



3.2.3 - The Influence of Ammonium Sulphate

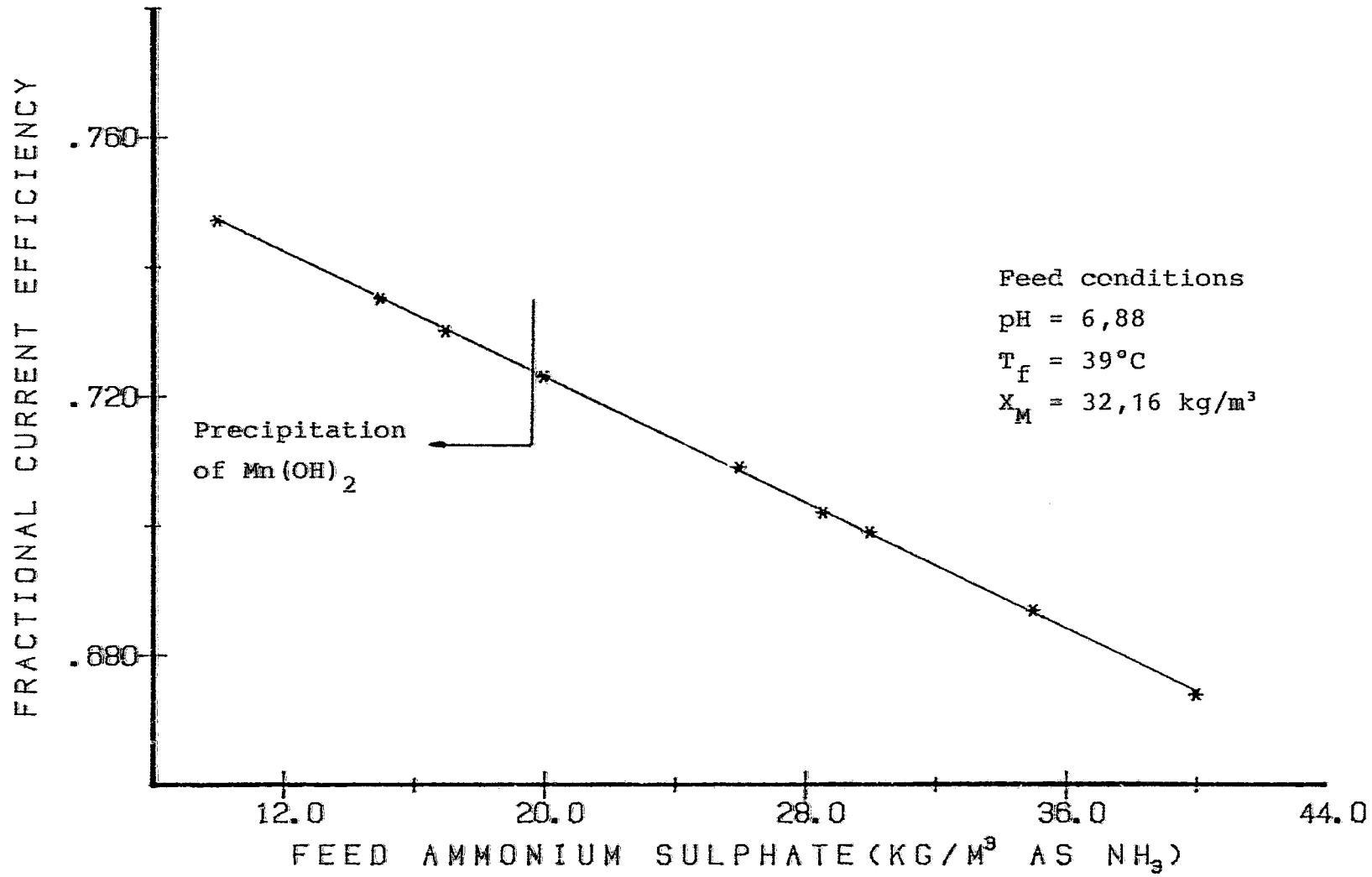
Ammonium sulphate is added to the electrolyte to increase the conductivity and also to buffer the solution,as mentioned in section 1.3.2

Figure 17 shows this influence,where a minimum amount of ammonium sulphate is required before the buffering action of this compound is felt , at a given catholyte pH.The fractional current efficiency decreases with increasing concentration of ammonium sulphate.Therefore the optimum lies in the interrelated effect of these two variables, as shown in section 3.2.7.

TABLE 9 - Ammonium Sulphate Concentration versus Fractional Current Efficiency

Concentration of Ammonium Sulphate (as NH_3 - kg/m^3)	Fractional Current Efficiency
10	0,747
15	0,735
17	0,730
20	0,723
26	0,709
28,57	0,702
30	0,699
35	0,687
40	0,674

FIGURE 17 - FRACT. CURRENT EFF. VS AMMONIUM SULPHATE CONC.



Feed conditions

pH = 6,88

T_f = 39°C

X_M = 32,16 kg/m³

3.2.4 - The Effect of Total Impurity Level on the Fractional Current Efficiency

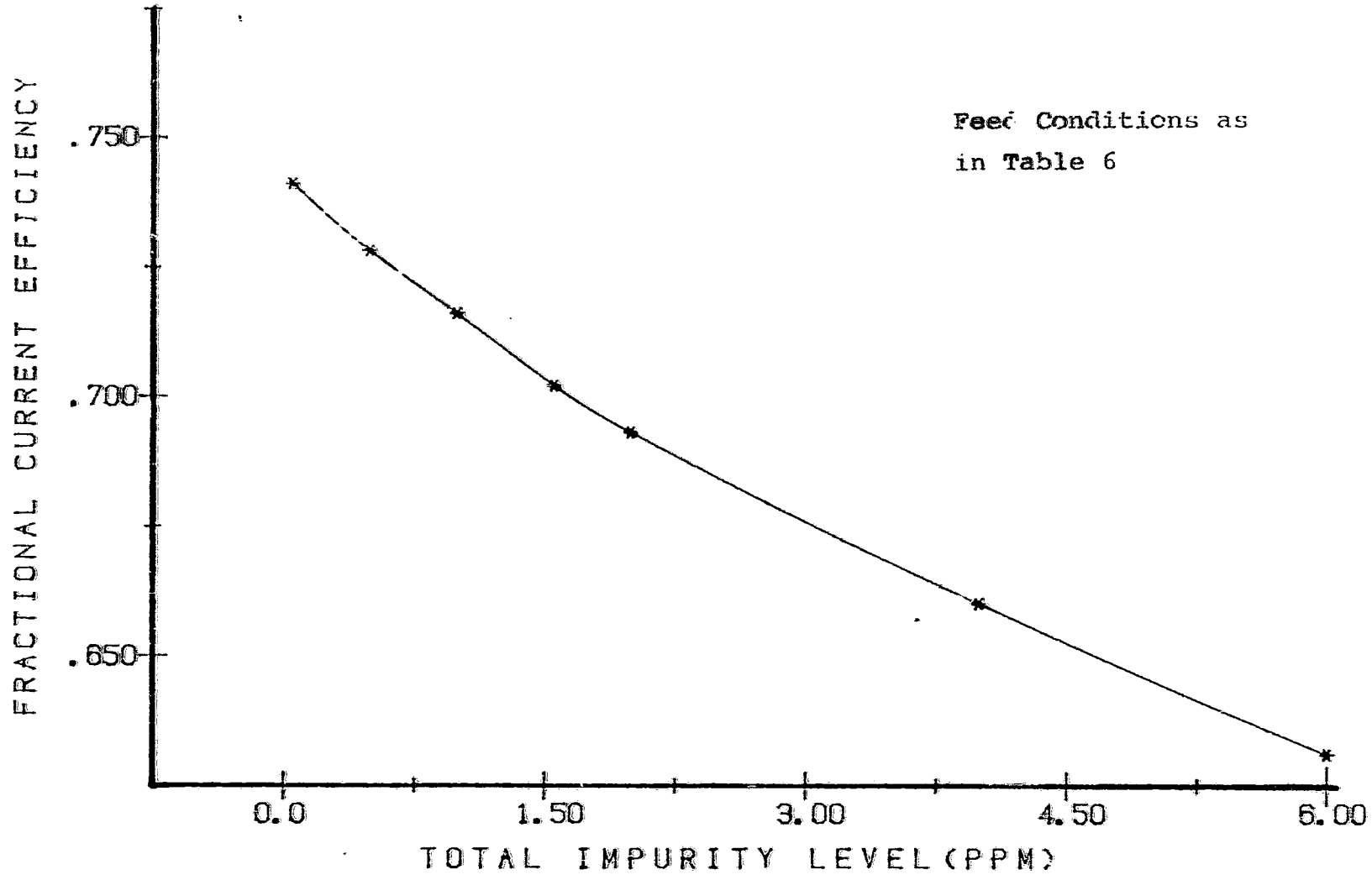
Figure 18 reveals that ultrapure electrolytes may not substantially increase the current efficiency.According to the model,by extrapolating the curve to 0 ppm of total impurity level,the maximum efficiency obtainable is 0,74 compared to 0,716 for a total impurity level of 1ppm,as shown in Table 10.To reduce the impurity level from 3 ppm to 1 ppm can be achieved with relative ease in practice, but purification below a ppm would probably increase the cost of this operation to a level far beyond the possible benefits that could be achieved through marginally higher current efficiencies .

It should be noted that it was only possible to consider the effect of total impurity level,and not the effect of the individual impurities.

TABLE 10 - Fractional Current Efficiency versus Total Impurity Concentration

Fractional Current Efficiency	Total Impurity Level (ppm)
0,711	0,06
0,728	0,50
0,716	1,00
0.702	1,56
0,693	2,00
0,660	4,00
0,631	6,00

FIGURE 18 - FRACT. CURRENT EFF. VS TOTAL IMPURITY LEVEL



Feed Conditions as in Table 6

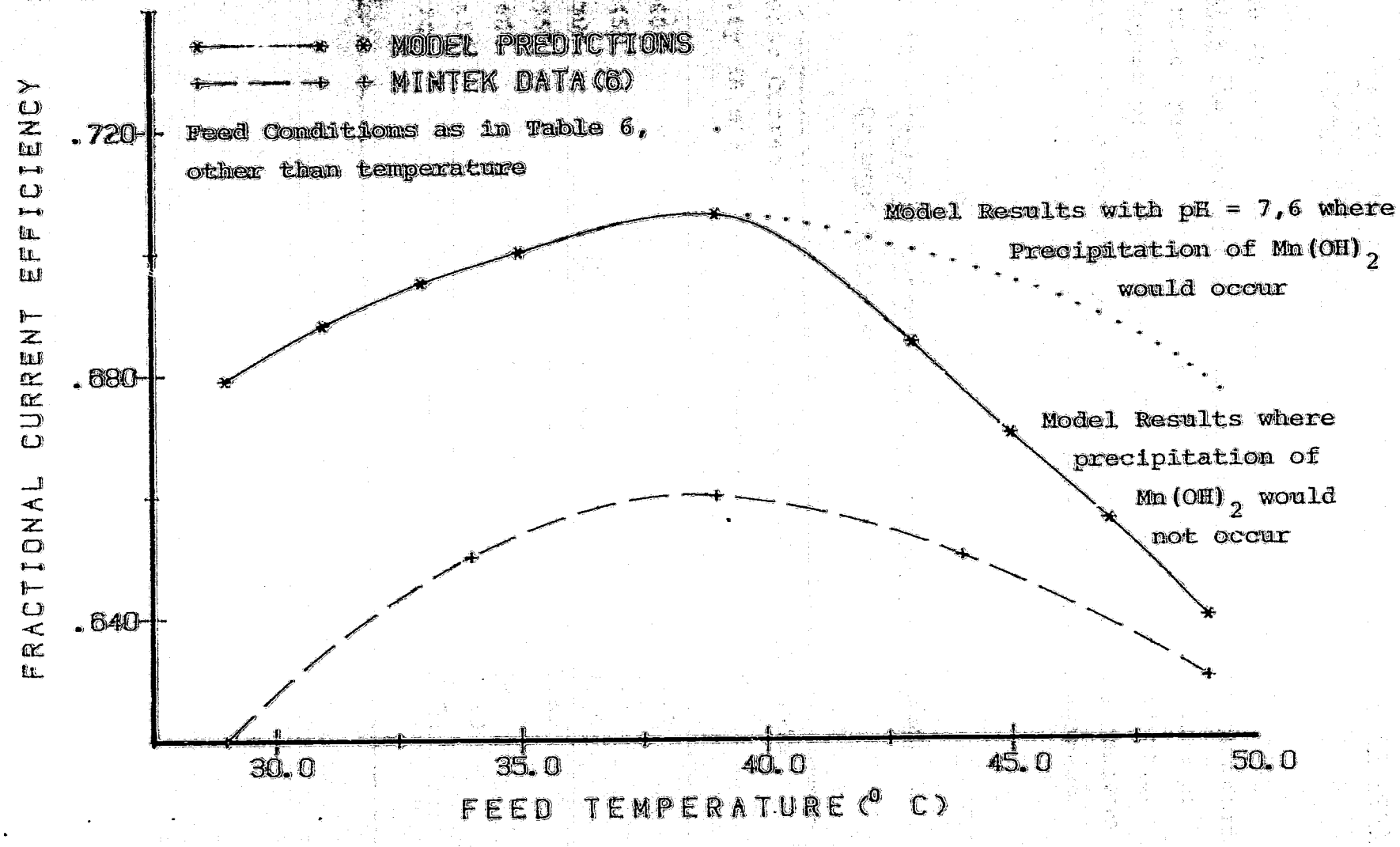
3.2.5 - The Effect of Feed Temperature on Fractional Current Efficiency

Temperature is known to be a very important parameter in the electrolytic deposition of manganese.Table 11 and Figure 19 show that,for every feed condition,there is an optimum temperature at which the current efficiency will be maximized.However,that optimum lies very near the point of manganese hydroxide $Mn(OH)_2$ deposition,as shown by the dotted line.The model,as it can be seen by Figure 19,shows a steeper loss of fractional current efficiency at higher temperatures due to the lowering of the lowest pH at which precipitation of $Mn(OH)_2$ will occur.The MINTEK (6) results are also plotted on the same graph,and again,the current efficiencies are always lower than the ones obtained at Delta, and predicted by the model.However the trend is the same as well as the optimum temperature reported.

TABLE 11 - Fractional Current Efficiency versus Temperature

Feed Temperature (°C)	Fractional Current Efficiency	Catholyte pH
29	0,679	7,6
31	0,688	7,6
33	0,695	7,6
35	0,700	7,6
39	0,706	7,63
43	0,685	7,5
45	0,670	7,45
47	0,659	7,4
49	0,640	7,3

FIGURE 19 - FRACT. CURRENT EFF. VS FEED TEMPERATURE



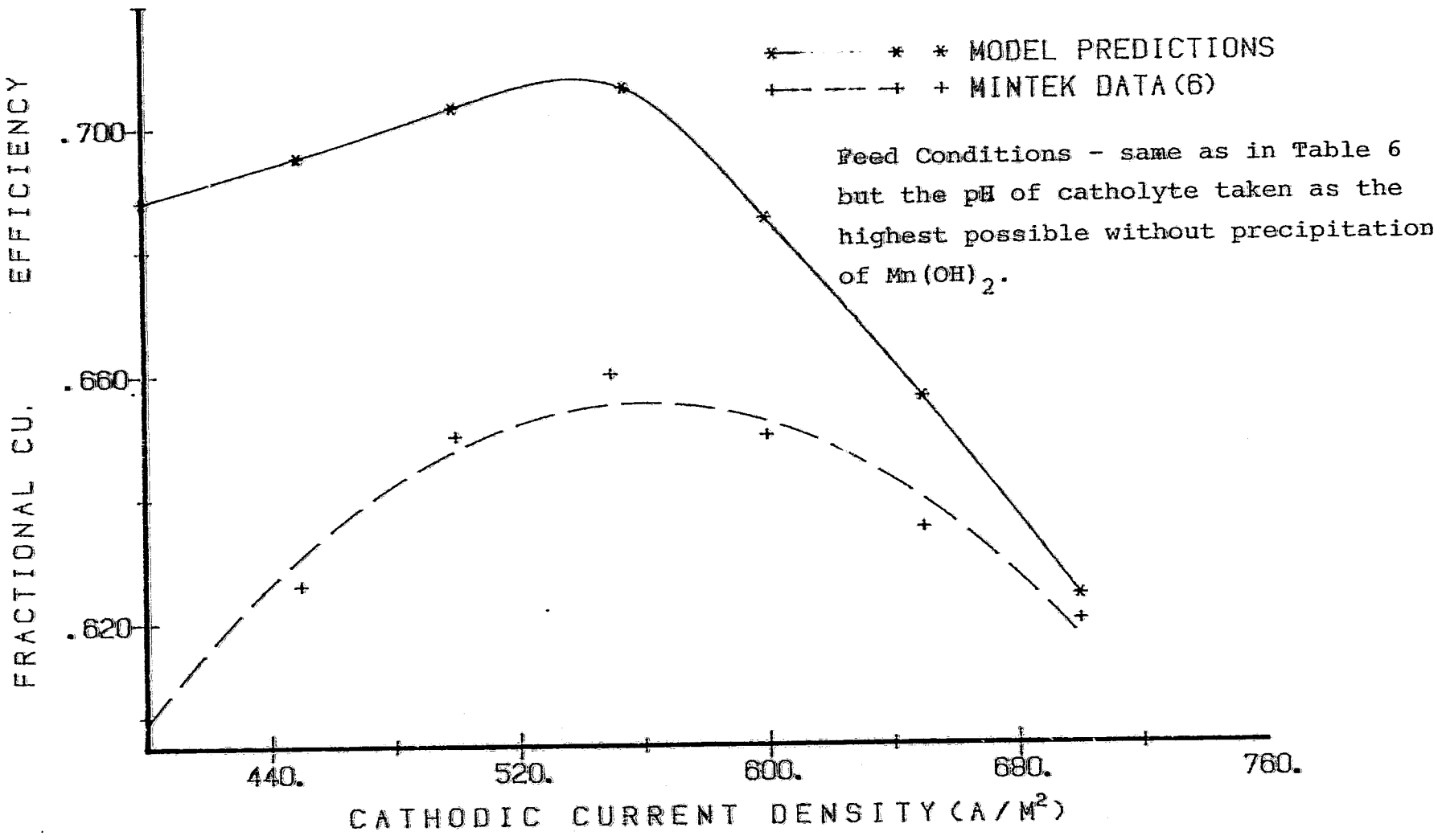
3.2.6 - The Effect of Cathodic Current Density on Fractional Current Efficiency

Figure 20 shows that there is an optimum current density at which the fractional current efficiency will be maximized. Both model prediction and the MINTEK (6) results agree on the figure of 550 A/m². When plotting the model prediction results, the catholyte pH was always chosen as the maximum value that could be used without precipitating manganese hydroxide.

TABLE 12 - Cathodic Current Density versus Fractional Current Efficiency

Cathodic Current Density (A/m²)	Fractional Current Efficiency	Catholyte pH
400	0,688	7,35
450	0,695	7,4
500	0,703	7,50
555	0,706	7,63
600	0,685	7,67
650	0,656	7,70
700	0,624	7,72

FIGURE 20 - FRACT. CURRENT EFF. VS CATH. CURRENT DENSITY



3.2.7 - The Limiting Catholyte pH versus the Ammonium Sulphate Concentration

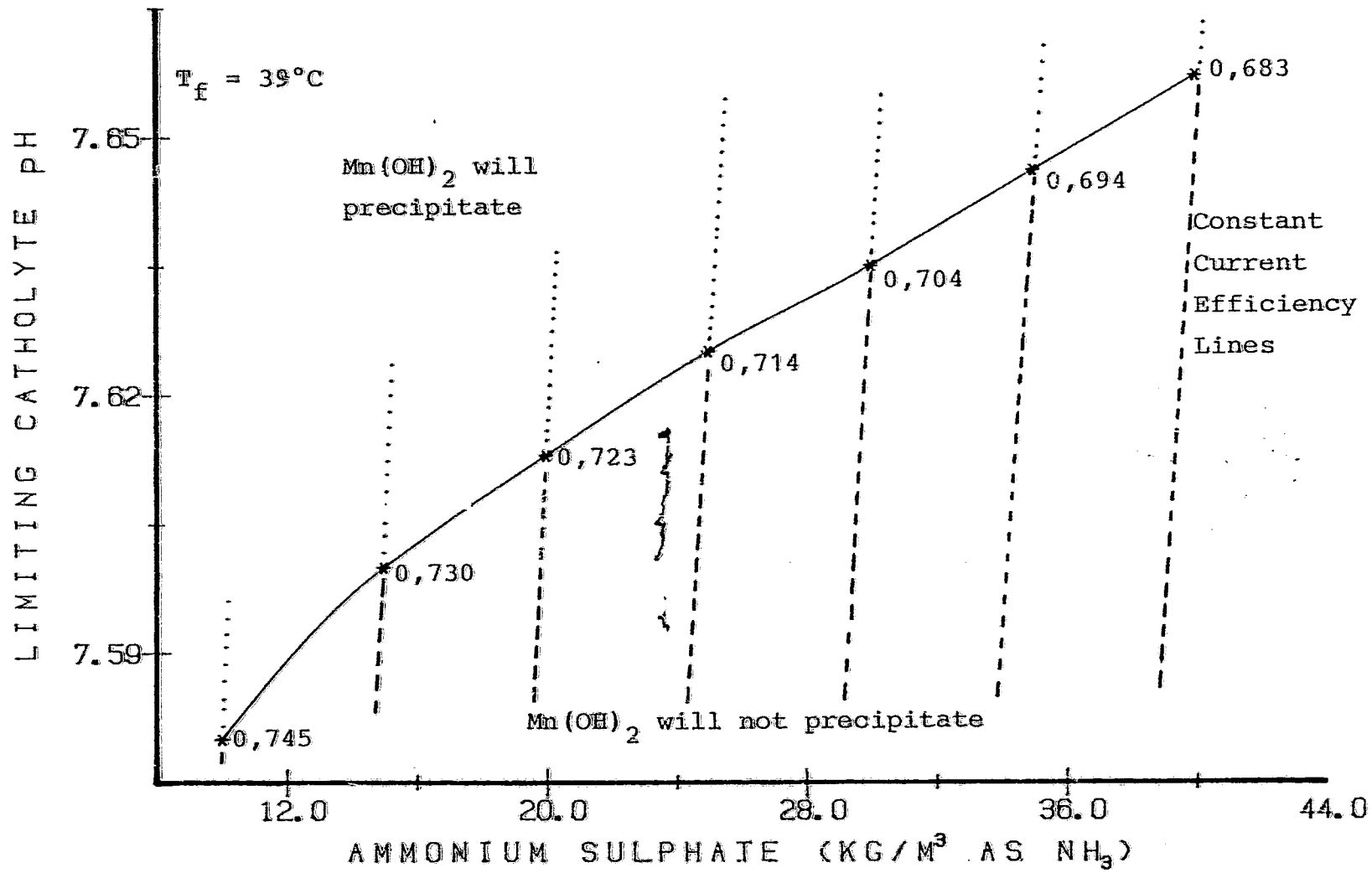
The limiting catholyte pH,i.e. the highest pH at which no manganese hydroxide precipitation will occur,is plotted against the concentration of ammonium sulphate, in Figure 21,showing the lines of fractional current efficiency.If no conductivity improvements were present by the addition of $(NH_4)_2SO_4$,the lower the concentration of this compound and the lower the pH would produce the highes current efficiencies.However it was found that the energy requirements outweigh this increase in cathodic current efficiency, and a minimum amount of ammonium sulphate is required.

Practice shows that an amount of 25 - .5 kg/m³ (given as NH_3) is required for the increase of electrical conductivity of the solution.

TABLE 13 - Limiting Catholyte pH versus Ammonium Sulphate Concentration

Ammonium Sulphate Concentration(kg/m³)	Limiting Catholyte pH	Fractional Current Efficiency
10 (as NH_3)	7,58	0,745
15	7,60	0,730
20	7,613	0,723
25	7,625	0,714
30	7,635	0,704
35	7,646	0,694
40	7,657	0,683

FIGURE 21 - LIMITING CATHOLYTE pH VS AMMONIUM SULPHATE CONC.



4 - REFERENCES

(1) Oliver and Boyd: 'Manganese Steel',Hadfield Ltd, London,1956

(2) Dean,Reginald S. : 'Electrolytic Manganese and its Alloys',New York,Ronald Press,1952

(3) Harris,M : Meyer D M :Auerswald K :'The Production of Electrolytic Manganese in South Africa',Journal of the S.A.Institute for Mining and Metallurgy,February 1977.

(4) Baggot, E.R. :'Electrowinning of Manganese Metal', SAIMM Electrometallurgy School,Randburg 1983, pp 203-235

(5) Woodman, F.W. and Jacobs, J.H. :'Studies in the Elec-deposition of Manganese',U S Bureau of Mines,1943, February,RI3681.

(6) Louis, P. and Martin, J.P. :'Increased Current Efficiency during the Electrodeposition of Manganese from Sulphate Electrolytes',MINTEK report no.1859,Randburg, South Africa 1976.

(7) Jacobs, J.H,Churchward P E,Knickerbocker R G :'The Effect of certain Variables on the Electrodeposition of Manganese' A paper presented at the 86th General Meeting held at Buffalo,N.York,October 14,1944 (US Bureau of Mines)

(8) Jacobs, J.H. :'The Effect of Cell Variables on the Electrowinning of Manganese' A paper presented at the 90th General Meeting held at Toronto, Canada,October 17,1946,(US Bureau of Mines)

(9) Tilak, B. V. K. et all :'Buffer Characteristics of Manganous Sulphate and Ammonium Sulphate Electrodeposition Baths' Trans.Faraday Soc. 58(1962) pp 795-804

(10) Kublanovskii, V. S. et all:'Mechanism of Electrodeposition of Manganese from a Sulphate Electrolyte',Institute of General and Inorganic Chemistry,Academy of Sciences of the Ukranian SSR,Kiev.Translated from Elektrokhimiya, Vol 11,no. 4,pp 586-589,April 1975.

(11) Tilak, B.V.K. et all: 'The Influence of Sulphur Dioxide on the Total and Partial Current-Potential Curves for the Electrodeposition of Manganese',ANN.SOC.CHIM. POLONORUM, 38,673,(1964)

(12) Shulyakas,A.K.et all:'Effect of Temperature on Electrodeposition of Manganese',Translated from Issled. Obl. Elektroosazwdneniya Met,Mater.Resp.Konf.Elektrokhim Lit. SSR,14th,1976. pp 116-119

(13) Cook, P.G:'A Mathematical Model of a Diaphragm-Type Chlor-Alkali Cell', A dissertation for a Masters Degree submitted to the University of the Wiwatersrand, Johannesburg,1978

(14) Bryson, A.W:'Modelling the Performance of Electrowinning Cells',Proceedings 'Hydrometallurgy 81',Society of Chemical Industry,London 1981,pp G2.1-G2.11

(15) Bates, R.G.:'Determination of pH',2nd Ed.,John Wiley and Sons Inc. New York,N.Y. 1973

(16) Weast,R.C.:'Handbook of Chemistry and Physics' ,CRC Press,57th Edition,Cleveland 1976/77

(17) Young,F.Thomas:'Recent Development in the Study of Interactions between Molecules and Ions of Equilibria in Solution',Record of Chem.Progress,12,no.2,1951

(18) Bryson,A.W.:Lawrence,M.G. : 'Ionic Transport in the Diaphragm of a Chlor-Alkali Cell',Chem.Eng.Commun., 1979,3,pp 53-58

(19) Stephen,K. and Vogt,H. : 'A Model for Correlating Mass Transfer Data at Gas Evolving Electrodes',Electrochimica Acta 24,(1979), pp11-18

(20) Latimer,W.M. :'The Oxidation States of the Elements and their Potentials in Aqueous Solutions',2nd Edition, Prentice Hall,Inc. Englewood Cli-fs,N.J. 1952

(21) Hurlen,T. and Valand,T. :'Activation Energy of the Mn/Mn^{2+} Electrode',Electrochimica Acta,9,1964 , pp1987-1092

(22) Nichol,M.J. :'Fundamentals of Electrochemistry',in Vacational School- Hydrometallurgy,SAIMM,Johannesburg, South Africa,1976

(23) Mayhew,Y.R. and Rogers,G.F.C. :'Thermodynamic and Transport Properties of Fluids',2nd Ed.,Basil Blackwell , Oxford 1977

(24) Perry,R.H. and Chilton,C.H. :'Chemical Engineering Handbook',5tn Edition,Mc Graw-Hill,Kogakusha,Ltd.

(25) Barner,H.E. and Scheuerman,R.V. : 'Handbook of Thermo-chemical Data for Compounds and Aqueous Species',John Wiley and Sons,New York N.Y. 1978

(26) Naumov,G.B.;Ryzhenko,B.N. and Khodakovsky,I.L. : 'Handbook of Thermodynamic Data',National Technical Service,US Department of Commerce,Springfield,VA.1974.

(27) Barin,I. and Knacke,O. :'Thermochemical Properties of Inorganic Substances',Springer-Verlag,Berlin. 1973.

(28) Newman,John: 'Electrochemical Systems',Englewood Cliffs, New Jersey:Prentice-Hall Inc. 1973

(29) Picket,D.J. :'Electrochemical Reactor Design',2nd Ed., Amsterdam,Elsevier Scientific Publishing Co. ,1979.

(30) Bryson,A.W.:Cook,P.G. and Lawrence,M.G.:'Ionic Transport in the Diaphragm of a Chlor-Alkali Cell',Chem.Eng. Commun.,1979,3,pp 53-58

(31) Jones,C.J.:'Continuous Leaching of a Reduced Manganese Ore',A dissertation submitted for a Masters Degree (Eng) at the University of the Witwatersrand,Johannesburg,1983.

APPENDIX A

Computer Model

```
200:REM  MAN6
210:REM  ******
220:LPRINT "MAN6AMLLE
230:LPRINT "******
240:LF 1
250:REM  OVERALL MASS BALANCE
260:D1=(1!85!*2*( AS(1.5-A
270:REM  D1,D2,D3 ARE THE FEED, PRODU
    CE AND CATHODE FE IN KG/M3
280:  PRINT  CATHODIC EFF
290:P2=.19
291:REM  IMPURITY  LEVEL IN CATHOL FE
     IN KMOL/M3
292:INPUT  "IMPURITY IN PRODUCTION
293:C0=C10.66666
295:REM  START OF LOOP
310:A4=0:H4=6.
311:E6=6. A
320:REM  FEED TEMP
330:INPUT "FEED TEMP.
340:INPUT "FEED PH
350:INPUT "FEED FE
360:INPUT "FEED AMMON
370:INPUT "FEED
380:REM  TOTAL EQUATION
390:I=.66666
400:REM  FEED EQUILIBRIUM
410:"=I
420:H=H1/84.34
430:H=H1:I7
440:F=P1
450:"=I+323
460:"=I
470:P2=12=(-P)
480:K1=EXP (-34.534.A5.I)
490:K2=EXP (40.32-.0641I)
500:J=. (1+I/(K2*K2))
510:A=(A-B)*P
520:A=A*K1.^2
530:P=A*K1/K2+1
540:"=A-Z*(Z*Z+4*.8*
550:P=A*K2/P
560:A=A-B
570:B=A*Z/(K2*P)
580:B=A*1.5*P*4
590:A=.21-54.1*P
    2*P5-.8*P8/.19
600:LPRINT "D1=
610:LPRINT "D2=
620:LPRINT "D3=
630:LPRINT "FEED
640:LPRINT "FEED
650:LPRINT "FEED
661:LF 1
670:LPRINT "FEED
675:LF 1
680:LPRINT "PH2=
685:LPRINT "PH4=
700:LPRINT "[PH4]2=
710:LPRINT "PH2=
720:LPRINT "[SO4]=
730:LPRINT "H2O=
740:LPRINT "MOL IN ATOL/M3"
741:LF 1
800:REM  DO THE LOOP
810:I=I+E8
820:A4=A4+H4*E6
830:A4=A4*84.34
840:A5=A4*E6
```

Computer Model (continued)

```
900:REM  OVERALL MASS BALANCE
910:T4=T1:GOSUB
920:REM  MASS&ENERGY BALANCE
930:REM  MANGANESE RECOVERED (M
    EQ) IS M1
940:M1=.82247*E1!!!
950:REM  H2 LIBERATED (M2) KG/S
960:M2=.08!*(1-E
970:REM  O2 LIBERATED (M3) KG/
980:M3=.089*E2!!
990:REM  MNO2 DEPOSITED (M4) KG/S
1000:M4=.0434*(1-E2)*!!
1010:O2=(O1*O1-M1-M2-M3-M4-M5-M
    1/O2
1020:REM M2=ANOLYTE MN;M3=ANOL
    MMONIA KG/M3
1030:M2=(*O1*O1-M1-M4)/32
1040:O3=(O1*O1-M4)/O2
1050:REM  ANOLYTE EQUILIBRIUM
1060:REM  ENERGY BALANCE ASSUMPTION
1070:T2=T1+3.5
1080:T=.273+T2
1090:TA=T
1100:K4=EXP (8.335-.0294*T.
1110:S=O1*F6/O2
1120:B1=M2/84.34
1130:B2=O3/17
1140:U=2*O1-B3-S+K4
1150:W=(2*S-2*O1-2*B2)*K4
1160:B2=(-U+(.U*U+4*2*O1)^.5)/2
1170:B6=2*O1+B2+B3-S
1180:B2=B-B6
1190:B6=(O2-94.34*O1-18*B3-36*BA-1
    6*B2)/16
1200:REM  DIAPHRAM MODEL
1210:REM  CATHOLYTE TEMP. FROM ENER
    GY BALANCE
1220:T4=T1+1.273
1230:TC=T
1240:TJ=T1+1
1250:M4=B1*84.34
1260:A=B3/17
1270:Z1=.02*E2*(2*O1-B3-S+K4)*.5*(4-E
    2*E2*!)/(2*E2
1280:Z2=.02*B2
1290:Z3=.02*(B2+B3)-.02*E2*(.5*(4-E2
    *E2*!)/(2*E2
1310:TP=1!*T*.0821
1320:PW=(1!*P*.0821/(.5*.3*(1+E2*!)-.28*.3
    *B2/.0409999999)
1330:J2=EXP (.051*.0068183
1340:A=.02*E2*J2+.02*(J2-1)*(.051/.00999999
    9*!)
1350:TCD=1!P/100.0
1360:'OR (PW=1!G 250
1370:P=P-.01
1380:P=P2
1390:C2=1@^(-P)
1400:K1=EXP (-24.53+.05*!)
1410:K2=EXP (48.32-.065*!
1420:K3=EXP (-65.124+.18253*!)
1430:W=1/(1+1/(K2*C2))
1440:W=(A-P)*W
1450:W=W*K1*C2
1460:P=W*K1*C2+1
1470:C1=(-Z+(Z*Z+4*K3*P)^.5)/(2*P)
1480:C3=K3*C1^2
1490:C4=P-C1
1500:C5=C3/(K2*C2)
1510:Y3=1.-.0075
1520:M=.2*C3/K3-C1
1530:C6=C1+.5*C5+C4
1540:IF M>0!THEN 4070 2050
1550:NEXT !PH
1560:LPRINT "PH(TM)2 WILL NOT PRECI
    PITATE"
2.05:REM  KINETIC MODEL
2110:I1=1+1000*C6/C1
2120:I2=14EXP (12368/(-48.05)
2130:I3=1-.008!3133*(!*CD-550.+.0099
    1270*(!*CD-550.)/(!*CD-550)
2140:C8=!/(1+1000000*J.*J2*J3*C2/C1
    )
2150:CED=885 (E0-E1)
2160:'P CED(.0005!THEN 40 0 2500
2161:S2M=B2/(271.806)
2162:S3M=B3/(2716)
2170:YBC=-1.287+.004287*!
2180:'BA=-1.287+.004287*A
2190:S4CAL=(Y3*(1-YBC-Y)  M2/M1)
2200:S4CAL=(YBC/(1-YBC-Y)  M2/M1)
2210:S5CAL=(B6/(1-Z6A)  M1/M1)
2220:GOTO 600
```

Computer Model(continued)

```
2500:REM  PRINTING ALL RESULTS
2510:LPRINT
2520:LPRINT "ANOLYTE CONDITIONS"
2521:LPRINT
2530:LPRINT "DISCHARGE RATE= ";D2
2540:LPRINT "ANOL.IONS=";M2
2550:LPRINT "ANOL.ACTION;a=";A2
2551:"2a=LOG (B2)
2560:LPRINT "ANOLYTE PH=";P2
2570:LPRINT "ANOLYTE TEMP=";T2
2580:LPRINT "ANOLYTE SUM CONCN;MA
     IONS"
2590:LPRINT "MN2+=";M1
2600:LPRINT "MH+ ";H2
2610:LPRINT "MNH4+ ";N2
2620:LPRINT "MSO4)2-=";S6
2630:LPRINT "MCl-=";C2
2640:LPRINT "M2O=";W8
2650:LPRINT
2660:LPRINT "DIAPHRAGM MODEL FLOWS"
2670:LPRINT
2680:LPRINT "M2O=";T8
2690:LPRINT "MN2+=";T1
2700:LPRINT "MNH4+=";T3
2710:LPRINT "MH+=";T2
2720:LPRINT
2730:LPRINT "CATHOLYTE CONC.CONS.="
     ;TCO
2740:LPRINT
2750:LPRINT "CATHOLYTE CONDITIONS"
2760:LPRINT "CATH.IMPULSE EL PPL=";I
     8
2770:LPRINT "CATH.MOLS.=";M
2780:LPRINT "CATH.TEMP.=";T
2790:LPRINT "CATH. PH=";P3
2800:LPRINT "MN2+=";I
2810:LPRINT "MH+=";I2
2820:LPRINT "MNH4+=";I3
2830:LPRINT "MNH4)2+=";I4
2840:LPRINT "MNa+=";I5
2850:LPRINT "MSO4)2-=";I6
2860:LPRINT "MH2 GAS FRACTION=";V3
2870:LPRINT "MH-DIFF.=";N
2880:LPRINT "ASS.CURR.EFF.=";E1
2890:LPRINT "ALK. WR.EFF.=";E2
2900:LPRINT "AMMONIA LOSSES=";H4
2910:LPRINT "WATER LOSSES CATH.=";A
     4
2920:LPRINT "WATER LOSSES ANOL.=";
     A5
2930:END
```

APPENDIX B

Typical Mass Balance Calculations

Given : T_f =39°C =312 K
pH_f = 6,88
X_M =32,16 kg/m³ = 0,5854 kmole/m³
X_A =28,57 kg?m³ = 1,6806 kmole/m³
Q_F =0,000552 m³/s = 1,9872 m³/h:
ξ_a = 0,99
ξ_c = 0,702

Basis - 1 hour

Total Mass input = 1185 x 1,9872 = 2354,8320 kg?hr

TABLE 14 - Feed Input - Mass Balance

Component	Concentration kmole/m³	kmoles/hr	Kg/hr
Mn^{2+} (aq)	0,5399	1,0610	58,2895
H^+ (aq)	$1,3182 \times 10^{-7}$	0,0000	0,0000
NH_4^+ (aq)	1,6114	3,2022	57,6396
$MnNH_3^{2+}$ (aq)	0,05147	0,1023	7,3581
NH_3 (aq)	0,01772	0,0352	0,5986
SO_4^{2-} (aq)	1,39106	2,7643	265,5445
HSO_4^- (aq)	-	-	-
Impurities	-	-	-
H_2O (aq)	54,9509 *	109,0963	1965,4017
TOTAL		116,2613	2354,8320

* The ion concentrations were calculated as in Appendix B.1

TABLE 15 - Products - Mass Balance

Components	kmoles/hr	kg/hr
Mn(s)	0,7333	40,2864
H_2(g)	0,3113	0,6275
O_2(g)	0,5171	16,5452
MnO_2(s)	0,0145	1,2609
	1,5762	58,8200

These figures are calculated using the equations below

$$P_{Mn} = \frac{\xi_c \, I}{2 \, F} \cdot 54,94 \times 10^{-3} \ (kg/s) \qquad (2.58)$$

$$P_{H_2} = \frac{(1 - \xi_c) \, I}{2 \, F} \cdot 2,0139 \times 10^{-3} \ (kg/s) \qquad (2.59)$$

$$P_{O_2} = \frac{\xi_a \, I}{4 \, F} \cdot 31,9988 \times 10^{-3} \ (kg/s) \qquad (2.60)$$

$$P_{MnO_2} = \frac{(1 - \xi_a) \, I}{2 \, F} \cdot 86,9388 \times 10^{-3} \ (kg/s) \qquad (2.61)$$

In this typical set of results, using I = 56000 A

P_{Mn} = 0,0112 kg/s = 40,2864 kg/hr

P_{H_2} = $1,7431 \times 10^{-4}$ kg/s = 0,6275 kg/hr

P_{O_2} = 0,0046 kg/s = 16,5452 kg/hr

P_{MnO_2} = $3,5026 \times 10^{-4}$ kg/s = 1,2609 kg/hr

TABLE 16 - Losses - Mass Balance

Components	kmoles/hr	kg/hr
H_2O(catholyte)	0,03276	0,59026
H_2O(anolyte)	0,04051	0,7297
NH_3(catholyte)	0,10699	1,8188
TOTAL	0,18026	3,13876

These losses are calculated using the equations in section (2.6),i.e. equations(2.50)to(2.55).These yield the following figures for the typical values:

$$Y_3 = 1,09817 \times 10^{-3}$$
$$y_3 = 2,3720 \times 10^{-3}$$
$$T_c = 40°C = 313K$$
$$Y_o = z_0 = 0,07264$$

Thus

kmoles H_2O lost from catholyte = 0,03276 kmoles/hr
= 0,59026 kg/hr

kmoles NH_3 lost from catholyte = 0,10699 kmoles/hr
= 1,81883 kg/hr

kmoles H_2O lost from anolyte = 0,04051 kmoles/hr
= 0,7279 kg/hr

Anolyte Discharge

Section 2.7 explains how the mass balance is performed in order to calculate the anolyte discharge.Equation(2.57) is the overall mass balance equation,and yields,with an anolyte density of 1160 kg/m³,and the values from Tables 15 and 16

$$\rho_a Q_a = 2293,1732 \text{ kg/hr}$$

$$Q_a = 1,9769 \text{ m}^3/\text{hr}$$

For each component,namely manganese , ammonia and sulphate, a mass balance is also performed to determine the total amounts of the above species present in the anolyte.These are:

Manganese Balance

$$54,94 \times Z_M Q_a = 54,94 X_M Q_f - P_{Mn} - P_{MnO_2}$$

Ammonia Balance

$$17,0 \times Z_A Q_a \; 0 \; 17,0 \times X_A Q_f - L_{NH_3}$$

Sulphate Balance

$$(Z_6 + Z_7) \times Q_a = X_6 Q_f$$

In this typical example,these equations yield

$Z_M = 0,2089$ kmole/m³

$Z_A = 1,6356$ kmole/m³

$Z_6 + Z_7 = 1,3983$ kmole/m³

Using the method explained in Appendix B.2 the various anolyte species concentrations are determined, and then, their individual discharge rates calculated, as shown in Table 17 below

TABLE 17 - Anolyte Discharge - Mass Balance

Component	Concentration (kmole/m³)	kmoles/hr	kg/hr
Mn^{2+} (aq)	0,20887	0,4129	22,6856
H^{+} (aq)	0,22841	0,4515	0,4551
NH_4^{+} (aq)	1,63560	3,2334	58,2015
NH_3 (aq)	-	-	-
$MnNH_3^{2+}$ (aq)	-	-	-
SO_4^{2-} (aq)	0,88344	1,7465	167,7689
HSO_4^{-} (aq)	0,51488	1,0179	98,8029
Impurities	-	-	-
H_2O (aq)	54,67238	107,9782	1945,2591
Total		114,8404	2293,1732

The following Table can be constructed using all the previous results, from Tables 14 to 17 .

TABLE 18 - Summary of the Overall Mass Balance

Description	IN		OUT	
	Kmoles/hr	kg/hr	kmoles/hr	kg/hr
Feed Input				
$Mn^{2+}(aq)$	1,0610	58,2895		
$H^{+}(aq)$	0,0000	0,0000		
$NH_4^{+}(aq)$	3,2022	57,6396		
$MnNH_3^{2+}(aq)$	0,1023	7,3581		
$NH_3(aq)$	0,0352	0,5986		
$SO_4^{2-}(aq)$	2,7643	265,5445		
$H_2O(aq)$	109,0963	1965,4017		
	116,2613	2354,8320		
Products				
$Mn(s)$			0,7333	40,2864
$H_2(g)$			0,3113	0,6275
$O_2(g)$			0,5171	16,5452
$MnO_2(s)$			0,0145	1,2609
			1,5762	58,8200
Losses				
H_2O(catholyte)			0,03276	0,59026
H_2O(anolyte)			0,04051	0,72970
NH_3(catholyte)			0,10699	1,81880
			0,18026	3,13876
Anolyte Discharge				
$Mn^{2+}(aq)$			0,4129	22,6956
$H^{+}(aq)$			0,4515	0,4551
$NH_4^{+}(aq)$			3,2334	58,2015
$SO_4^{2-}(aq)$			1,7465	167,7689
$HSO_4^{-}(aq)$			1,0179	98,8029
$H_2O(aq)$			107,9782	1945,2591
			114,8404	2293,1732
TOTAL(to the nearest integer)	116	2355	116	2355

Calculating the Catholyte Conditions

The catholyte temperature is estimated using the approximations

$$T_c = 0,7\ T_f + 0,3\ T_A \qquad (2.69)$$

Once the temperature is known,then the catholyte conditions are determined using the diaphragm model and the equilibrium ratio equations (2.2),(2.4) and (2.6).The method is the same as for the feed condtions,as explained in Appendix B.1.

Using equation (2.13) , with $Y_2 \simeq 0$ the following values for Y_a and W_2 are found

$$Y_a = 1,9723 \text{ kmole/m}^3$$
$$W_2 = -1,779453\text{x}10^{-4} \text{kmole/s}$$

Now $Y_2 = 10^{-7,6}$,as this is the figure that balances W_2 with the amount of H^+ required to produce H_2 and to react in the equations below

$$NH_3 + H^+ \rightleftharpoons NH_4^+ \qquad (2.3)$$

$$MnNH_3^{2+} + H^+ \rightleftharpoons Mn^{2+} + NH_4^+ \qquad (2.1)$$

Now $Y_M \simeq Z_M$ and having this,the pH and Y_a it is possible to find the individual concentrations of the species using the same method as in Appendix B.1.

The typical catholyte concentrations then become:

$Y_1 = 0,13138$ kmole/m³
$Y_2 = 10^{-7,6}$ kmole/m³
$Y_3 = 1,784995$ kmole/m³
$Y_4 = 0,0775$ kmole/m³
$Y_5 = 0,10982$ kmole/m³
$Y_6 = 1,10136$ kmole/m³
$Y_8 = 2,6\text{x}10^{-2}$ kmole/m³

APPENDIX B.1

Solving for the Feed Ion Concentration

The following equations apply to the feed conditions,as they relate the individual ion concentrations to the total amounts of manganese and ammonia.

Manganese

$$X_M = X_1 + X_4 \qquad (B.1)$$

Ammonia

$$X_a = X_3 + X_4 + X_5 \qquad (B.2)$$

The electrical neutrality equation,as previously explained holds for the feed solution as well,and it is

$$2X_1 + X_2 + X_3 + 2X_4 - 2X_6 = 0$$

As $X_2 = 10^{-pH} \simeq 0$ when compared to the other concentrations,the above equation simplifies to

$$2X_1 + X_3 + 2X_4 - 2X_6 = 0 \qquad (B.3)$$

Solution Equilibria

At the feed, the equilibrium conditions as stated below apply

$$Mn^{2+} + NH_4^+ \underset{K_c'}{\rightleftharpoons} MnNH_3^{2+} + H^+$$

where

$$K'_c = \frac{X_2\ X_4}{X_1\ X_3} = \exp\ (-34{,}57 + 0{,}051\ T) \qquad (B.4)$$

$$NH_3 + H^+ \underset{K'_a}{\rightleftharpoons} NH_4^+$$

and

$$K'_a = \frac{X_3}{X_2\ X_5} = \exp(40{,}32 + 0{,}064\ T) \qquad (B.5)$$

The precipitation of manganese hydroxide $Mn(OH)_2$ is detrimental to the electrodeposition process

$$Mn^{2+} + 2\ H_2O \underset{K'_s}{\rightleftharpoons} Mn(OH)_2 + 2\ H^+$$

where

$$K'_s = \frac{X_2^{\ 2}}{X_{1s}} = \exp(-65{,}17 + 0.1025) \qquad (B.6)$$

Defining

$$\Delta X_1 = \frac{X_2^{\ 2}}{K'_s} - X_1$$

Then the precipitation of manganese hydroxide will occur if

$$\Delta X_1 < 0 \qquad (B.7)$$

Given equations (B.1) to (B.5) then it is needed to solve for X_1, X_3, X_4, X_5 and X_6. X_2 is known from the pH of the solution.

Method

$$X_2 = 10^{-pH}$$

Write X_3, X_4 and X_5 as functions of X_1. From equation (B.5) put $X_5 = f(X_3)$

$$X_5 = \frac{X_3}{K'_a\ X_2} \qquad (B.8)$$

Subtracting equation (B.2) from (B.1)

$$X_a - X_M = X_3 + X_5 - X_1$$

Substituting (B.8) in the above equation we obtain

$$X_a - X_M = X_3 + \frac{X_3}{K'_a\ X_2} - X_1$$

i.e.

$$X_a - X_M = X_3\left(1 + \frac{1}{K'_a\ X_2}\right) - X_1$$

Now let

$$U = \frac{1}{1 + \frac{1}{K'_a\ X_2}}$$

then

$$X_3 = \left[(X_a - X_M) + X_1\right].U \qquad (B.9)$$

From equation (B.1)

$$X_4 = X_M - X_1 \qquad (B.10)$$

Substituting in equation (B.4) we can solve for X_1 as follows:

Let

$$V = (X_a - X_M) \cdot U$$

and

$$W = \frac{U \cdot K'_C}{X_2}$$

and

$$Z = \frac{K'_C \cdot V}{X_2} + 1$$

the obtaining the following equation in X_1

$$W X_1^2 + Z X_1 - X_M = 0$$

which can be solved for X_1

$$X_1 = \frac{-Z + \sqrt{Z^2 + 4.W.X_M}}{2.W} \qquad (B.11)$$

Then equations (B.8), (B.9), (B.10) and (B.3) give X_4, X_3, X_5 and X_6 respectively.

Typical set of results

Using the following feed conditions

T_f = 39°C = 312 K
X_M = 32,16 kg/m³ = 0,5854 kmole/m³
X_a = 28,57 kg/m³ = 1,6806 kmole/m³
pH_f = 6,88

The ion concentrations of the feed will be

X_1=0,5333 kmole/m³ X_5=1,772 x 10^{-2} kmole/m³
X_3=1,6115 kmole/m³ X_6=1,3905 kmole/m³
X_4=0,0514 kmole/m³ X_2=1,3183 x 10^{-7} kmole/m³
ΔX_1=2,7833 > 0 i.e. $Mn(OH)_2$ will not precipitate

APPENDIX B.2

Solving for the Anolyte Concentrations

The following are the chemical reactions taking place in the anolyte, as previously cited.

$$HSO_4^- \underset{K_h'}{\rightleftharpoons} H^+ + SO_4^{2-}$$

where

$$K_h' = \frac{Z_2 \, Z_6}{Z_7} = \exp(8,339 - 0,0294\ T) \qquad (B.12)$$

All the other species NH_3 and $MnNH_3^{2+}$ do not exist in the anolyte, due to the pH. However, the component balances and electrical neutrality equation still apply.

Manganese Balance

$$Z_1 = Z_M \qquad (B.13)$$

Ammonia Balance

$$Z_3 = Z_a \qquad (B.14)$$

Sulphate Balance

$$S = \frac{Q_f \, X_6}{Q_a} \qquad (B.15)$$

and

$$S = Z_6 + Z_7 \qquad (B.16)$$

Electrical neutrality

$$2Z_1 + Z_2 + Z_3 - 2Z_6 - Z_7 = 0 \qquad (B.17)$$

Method for solving

The above equation (B.17) is solved for Z_6, using equation (B.16) as an intermediate, i.e.

$$Z_6 = 2Z_1 + Z_2 + Z_3 - S \qquad (B.18)$$

then, using equation (B.16) again and solving for Z_7 as a function of Z_2 gives

$$Z_7 = S - Z_6 = 2S - Z_1 - Z_2 - Z_3 \qquad (B.19)$$

Substituting equations (B.18) and (B.19) in equation (B.12) a quadratic in Z_2 is obtained as follows

$$Z_2 = \frac{-U + \sqrt{U^2 + 4V}}{2} \qquad (B.20)$$

where

$$U = 2Z_1 + Z_3 - S + K_h' \qquad (B.21)$$

and

$$V = (2S - 2Z_1 - Z_3) K_h' \qquad (B.22)$$

Once Z_2 is obtained from equation (B.20) then it is easy to calculate the other ion concentrations using equations (B.18) and (B.19), since Z_1 and Z_3 are obtained from equations (B.13) and (b.14) directly.

Typical Set of Results

In our example, the anolyte conditions become

$$Z_M = 11,475 \text{ kg/m}^3$$
$$Z_a = 27,805 \text{ kg/m}^3$$

and the individual ion concentrations are

$$z_1 = 0,2089 \text{ kmole/m}^3$$
$$z_2 = 2,2841\text{x}10^{-1} \text{ kmole/m}^3$$
$$z_3 = 1,6356 \text{ kmole/m}^3$$
$$z_6 = 0,8834 \text{ kmole/m}^3$$
$$z_7 = 0,51487 \text{ kmole/m}^3$$
$$z_0 = 54,6724 \text{ kmole/m}^3$$

Thus

$$pH_a = 0,6413$$

and

$$T_a = 42,5°C$$

APPENDIX C

Typical Energy Balance Calculations

The overall energy balance in kJ/s is

$$Q_f \Sigma X_f H_j + \frac{V I}{1000} = Q_a \Sigma Z_j H_j + \Sigma M_j H_j + q_c + q_l \qquad (2.64)$$

where

$$H_j = \Delta H^o_{fj} + (T - 298) C^*_{pj} \qquad (2.66)$$

Table 5 in section 2.8 gives Molar Enthalpies of Formation and Molar Specific Heats for the necessary species.

The energy removed by the cooling coils is given by

$$q_c = 4184 Q_c (T_2 - T_1) \qquad (2.67)$$

The plant data from Delta allowed the calculation of an empirical relationship between the feed and anolyte temperatures to estimate the catholyte temperature

$$T_c = 0,7 T_f + 0,3 T_a \qquad (2.69)$$

Using Table 14, from Appendix B, in conjunction with Table 5 in section 2.8, it is possible to calculate the Energy Input in the feed stream, using equation (2.66).

TABLE 19 - Energy Input in the Feed Stream

Component	$Q_f X_j$ kmoles/hr	$Q_f X_j \Delta H^0_{fj}$ kJ/hr x 10^{-3}	$Q_f X_j C^*_{pj} (T_o - 298)$ kJ/hr x 10^{-3}	$Q_f X_j H_j$ kJ/hr x 10^{-3}
Mn^{2+} (aq)	1,0610	233,9505	-2,7331	231,2174
H^+ (aq)	0,0000	0,0000	0,0000	0,0000
NH_4^+ (aq)	3,2022	424,6117	-5,2452	419,3665
$MnNH_3^{2+}$ (aq)	0,1023	30,7718	-0,2163	30,55555
NH_3 (aq)	0,0352	2,8266	0;0168	2,8434
SO_4^{2-} (aq)	2,7642	2513,2110	11,6483	2524,8593
HSO_4^- (aq)	-	-	-	-
Impurities	-	-	-	-
H_2O (aq)	109,0963	31179,7225	-114,55112	31065,1710
Total	116,2613			34274,014 (9520,5 kW)

Feed temperature taken as 39°C (i.e. 312K)

The power input term is

$$\frac{V\ I}{1000} \times 3600 = \frac{6,52 \times 56000 \times 3600}{1000} = 1,314432 \times 10^6 \text{ kJ/hr}$$

because the voltage is V = 6,52V and the current 56000A.

Thus the total energy input term is

$$35,588446 \times 10^6 \text{ kJ/hr } (9,8856794 \times 10^3 \text{ kW})$$

For an anolyte temperature of 42,5°C,a similar procedure is now followed to estimate the energy taken by the discharge stream.Tables 17(Appendix B) and 5(section 2.8) are used for this calculation ,as shown below in Table 20.

TABLE 20 - Energy Output through the Discharge Stream

Component	$Q_a \cdot Z_j$ Kmoles/hr	$Q_a Z_j \Delta H^{\circ}_{fj}{}_{-3}$ kJ/hr x 10^{-3}	$Q_a Z_j C^{*}_{pj} (T_a - 298)$ kJ/hr x 10^{-3}	$Q_a Z_j H_j$ kJ/hr x 10^{-3}
Mn^{2+}(aq)	0,4129	91,0444	-1,3295	89,7149
H^{+}(aq)	0,4515	0,0000	0,0000	0,0000
NH_4^{+}(aq)	3,2334	428,7488	-6,6204	422,1284
$MnNH_3^{2+}$(aq)	-	-	-	-
NH_3(aq)	-	-	-	-
SO_4^{2-}(aq)	1,7465	1587,9178	9,1997	1597,1175
HSO_4^{-}(aq)	1,0179	904,6077	1,2647	905,8274
Impurities	-	-	-	-
H_2O(aq)	107,9782	30860,170	-141,7214	30718,4486
Total	114,8404			33733,2819 (9,3704 x10^3kW)

Once the discharge stream enthalpy is estimated,there are other outlet enthalpies , namely the produced products and the ammonia and ammonia losses.Once again,using Table 5 and Tables 15 and 16,the energy term for these compounds is estimated and tabulated below (Table 21).

TABLE 21 - Energy Term from Products and Losses

Components	M_j kmoles/hr	$M_j \Delta H^0_{fj}$ kJ/hr x 10^{-3}	$M_j C^*_{pj}$ (T-298) kJ/hr x 10^{-3}	$M_j H_j$ kJ/hr x 10^{-3}
Mn (s)	0,7333	0,0000	-0,37398	-0,37398
H_2 (g)	0,3113	0,0000	-0,1538	-0,1588
O_2 (g)	0,5171	0,0000	-0,3077	-0,3077
MnO_2 (s)	0,0145	7,5415	-0,0127	7,5288
H_2O (g) catholyte	0,03276	7,9214	-0,0167	7,9047
H_2O (g) anolyte	0,04051	9,7953	-0,0241	9,7712
NH_3 (g) catholyte	0,10699	4,9215	-0,0546	4,8670
Total				29,2312
				(8,1422 kW)

The energy removed by the cooling coils is

$$q_c = 4184\ Q_c\ (T_2 - T_1)$$

where Q_c = 30,05 m^3/hr

T_2 = 306 K

T_1 = 292 K

Then q_c = 489,08 kW = 1760,688 kJ/hr

Thus the Energy Balance will be

TABLE 22 - Overall Energy Balance

	Energy IN (kJ/s)	Energy OUT (kJ/s)
Inlet Stream	9520,5	
Power Input	365,1	
Discharge Stream		9370,4
Products and Losses		8,1
Energy Removed from cooling coils		489,1
Energy lost to surroundings		18,0
Total	9885,6	9885,6

APPENDIX D.1

Modelling the Ammonia-Manganese Complex Reaction Equilibrium Ratio

The following are a Table of results obtained by directly measuring the concentration ratio for the reaction below at various temperatures

$$Mn^{2+} + NH_4^{+} \underset{K'_c}{\rightleftharpoons} MnNH_3^{2+} + H^{+}$$

where

$$K'_c = \frac{Y_2\ Y_4}{Y_1\ Y_3}$$

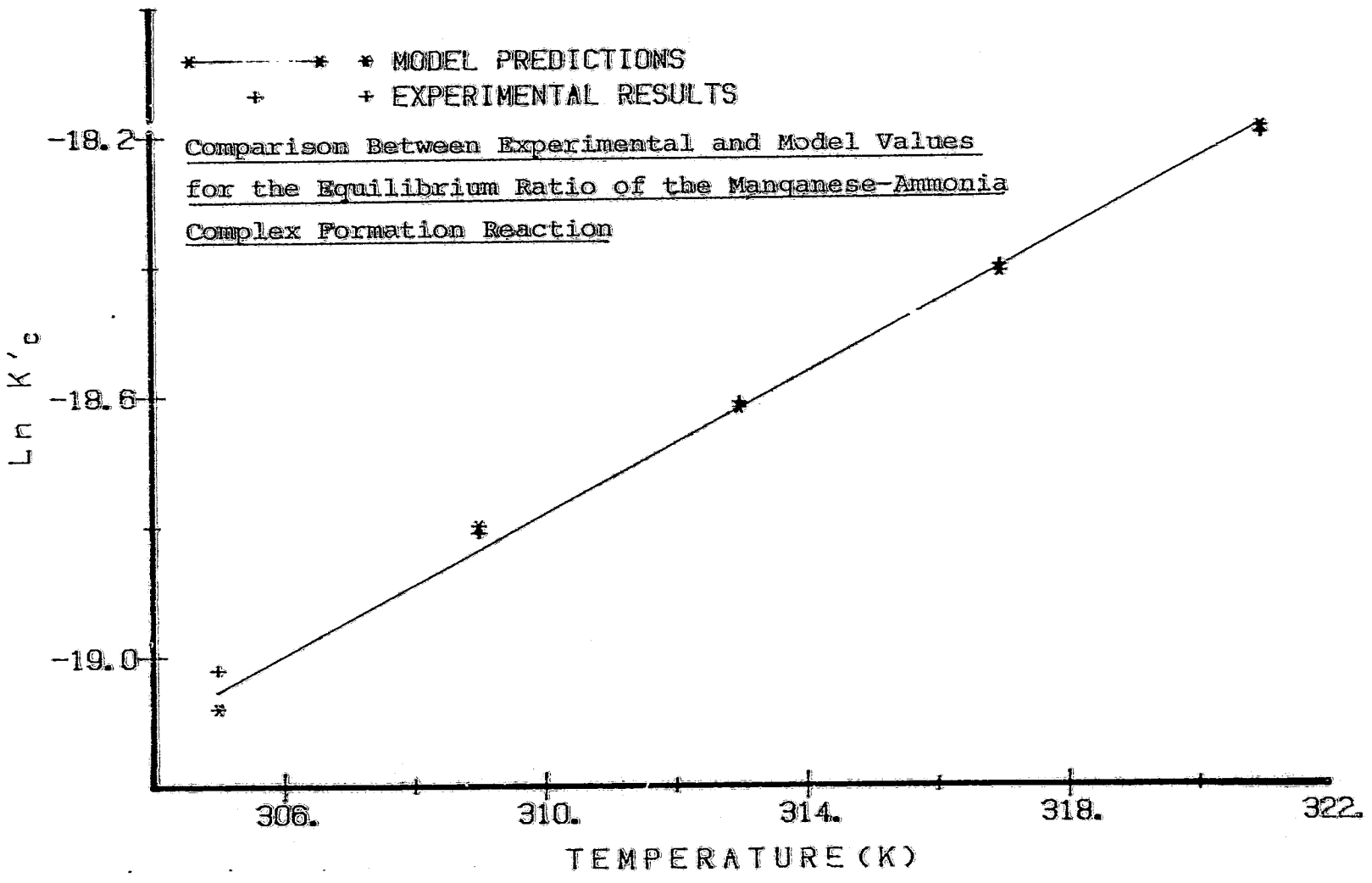
and has been modelled as

$$K'_c = \exp(-34{,}57 + 0{,}051\ T) \quad \text{for} \quad 295 < T < 330$$

TABLE 23 Experimental and Model values for the Manganese-Ammonia Complex Reaction Equilibrium Ratio

T		Experimental		Model	
°C	K	K'_c	ln K'_c	K'_c	ln K'_c
32	305	$5{,}181 \times 10^{-9}$	-19.08	$5{,}519 \times 10^{-9}$	-19,02
36	309	$6{,}81 \times 10^{-9}$	-18,80	$6{,}769 \times 10^{-9}$	-18,81
40	313	$8{,}19 \times 10^{-9}$	-18,62	$8{,}300 \times 10^{-9}$	-18,61
44	317	$10{,}10 \times 10^{-9}$	-18,41	$10{,}18 \times 10^{-9}$	-18,40
48	321	$12{,}61 \times 10^{-9}$	-18,19	$12{,}48 \times 10^{-9}$	-18,20

FIGURE 22



Comparison Between Experimental and Model Values for the Equilibrium Ratio of the Manganese-Ammonia Complex Formation Reaction

APPENDIX D.2

Modelling the Ammonium-Ammonia Equilibrium Ratio

The reaction between the ammonium ion and ammonia in the liquid solution has significance in the catholyte. The equilibrium ratio between the two species was modelled from the data supplied by Weast (16).

$$NH_3 + H^+ \underset{K'_a}{\rightleftharpoons} NH_4^+$$

$$K'_a = \frac{Y_3}{Y_5\ Y_1}$$

The model found to best fit the data in the range $295 < T < 330$ is

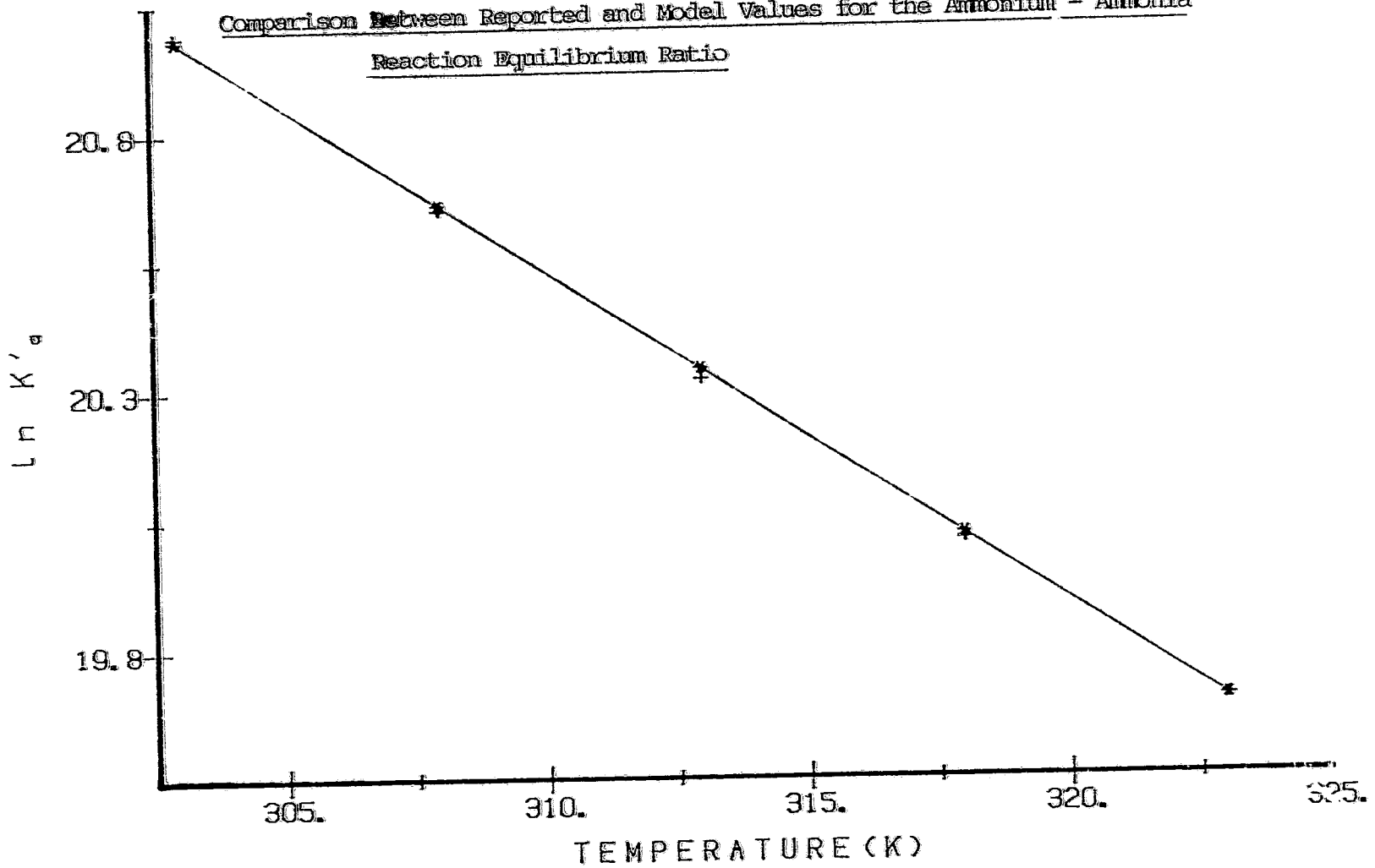
$$K'_a = \exp\ (40{,}32 - 0{,}064\ T)$$

TABLE 24 - Experimental and Model Values for the Ammonia-Ammonium Equilibrium Ratio

Temperature		Experimental		Model	
°C	K	K'_a	ln K'_a	K'_a	ln K'_a
30	303	$1{,}239 \times 10^9$	20,94	$1{,}227 \times 10^9$	20,93
35	308	$0{,}885 \times 10^9$	20,60	$0{,}891 \times 10^9$	20,61
40	313	$0{,}637 \times 10^9$	20,27	$0{,}647 \times 10^9$	20,29
45	318	$0{,}467 \times 10^9$	19,96	$0{,}470 \times 10^9$	19,97
50	323	$0{,}345 \times 10^9$	19,66	$0{,}341 \times 10^9$	19,65

FIGURE 23

Comparison Between Reported and Model Values for the Ammonium - Ammonia Reaction Equilibrium Ratio



APPENDIX D.3

Modelling the Solubility Product of Manganese Hydroxide

Manganese ion when reacting with the hydroxide ion producing manganese hydroxide,which precipitates if saturation is reached, does so according to the following reaction:

$$Mn^{2+} + 2OH^- \rightleftharpoons Mn(OH)_2$$

The solubility product K'_{sp} is defined as

$$K'_{sp} = \left[OH^-\right]^2 \left[Mn^{2+}\right]$$

However,in this study the hydrogen ion is required to be related to all other variables and it is convenient to express the solubility product in terms of $\left[H^+\right]$.This is done by defining the following equilibrium ratio

$$K'_s = \frac{\left[H^+\right]^2}{\left[Mn^{2+}\right]} = \frac{K'^2_w}{K'_{sp}}$$

where $K'_w = \left[OH^-\right]\left[H^+\right]$ is the equilibrium concentration product for the dissociation of water.Thus in terms of our nomenclature

$$K'_s = \frac{Y_2^2}{Y_1}$$

The model used for this newly defined equilibrium ratio is

$$K'_s = \frac{Y_2^2}{Y_1} = \exp(-65,17 + 0,1025\ T)$$

and by letting $\Delta Y_1 = \frac{Y_2^2}{K'_s} - Y_1$ precipitation of manganese hydroxide will occur if $\Delta Y_1 < 0$

TABLE 25 - Experimental and Predicted Values for the Manganese Hydroxide Formation Reaction Equilibrium Ratio

Temperature		Experimental	Model
°C	K	ln K'_s	ln K'_s
32	305	-37,07	-34,11
36	309	-36,75	-33,50
40	313	-36,33	-33,09
44	317	-35,92	-32,68
48	321	-35,51	-32,27

The experimental values in Table 25 are those determined by Bryson (unpublished data). These were evaluated with a 0,91 Molar $MnSO_4$ solution with no $(NH_4)_2SO_4$ present. The expression used in the model was adjusted because:

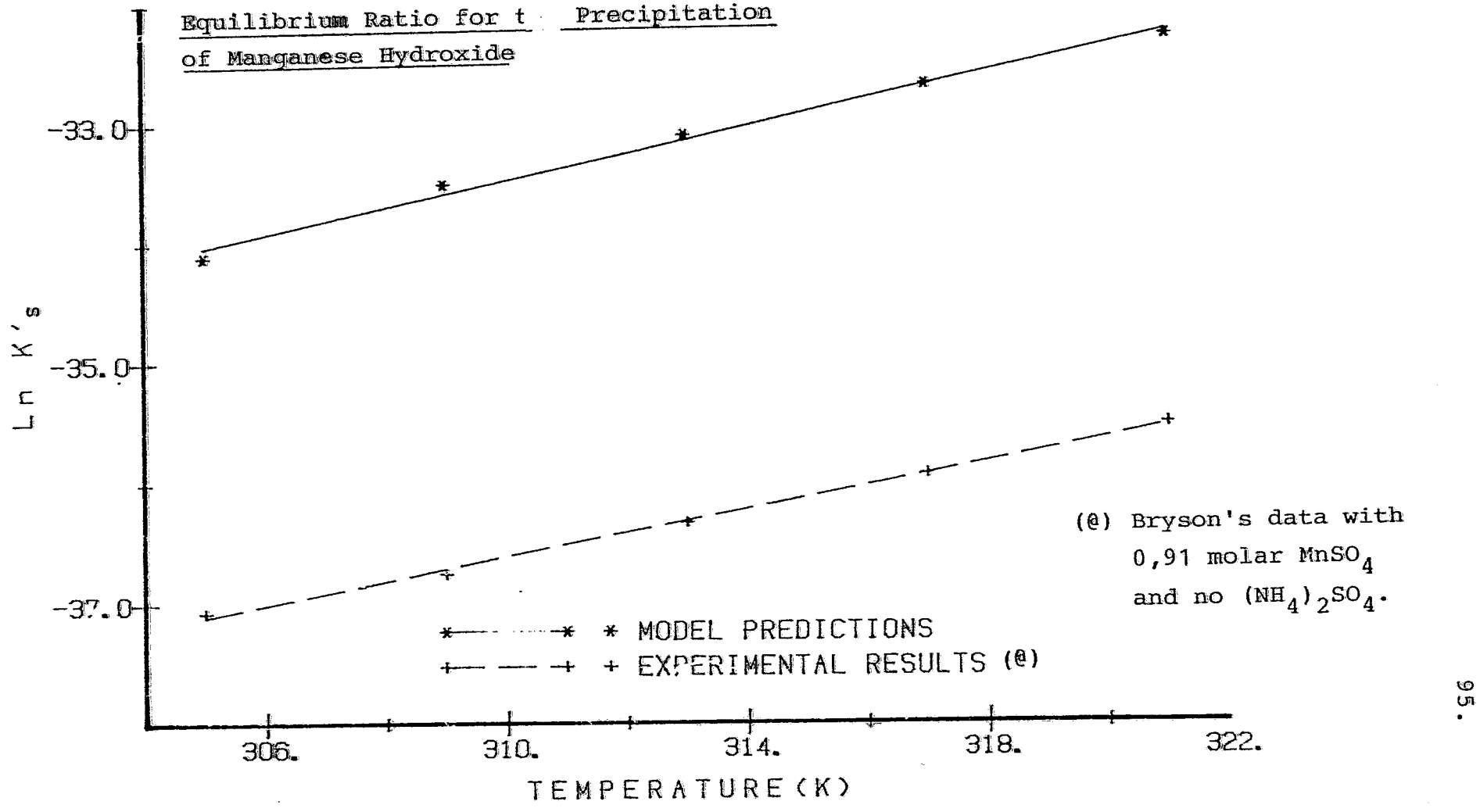
(i) The model results using the above expression fitted observed behaviour on the plant.

(ii) Jones (31) found that his results could best be simulated using

$$K'_s = \exp\ (-66,00 + 0,1025\ T)$$

(iii) The high sulphate content of the plant solution, compared to that used by Bryson, would result in lower manganese ion activity.

FIGURE 24


Equilibrium Ratio for t Precipitation
of Manganese Hydroxide
-33.0
-35.0
-37.0
Ln K's
306.
310.
314.
318.
322.
TEMPERATURE (K)
* MODEL PREDICTIONS
+ EXPERIMENTAL RESULTS (@)
(@) Bryson's data with
0,91 molar $MnSO_4$
and no $(NH_4)_2SO_4$.

APPENDIX D.4

Modelling the Sulphate-Bisulphate Equilibrium Ratio

At the low anolyte pH's ,the ionic species present in the electrolyte change drastically from those present in the feed and catholyte due to the sulphate-bisulphate equilibrium

$$HSO_4^- \rightleftharpoons SO_4^{2-} + H^+ \qquad (2.8)$$

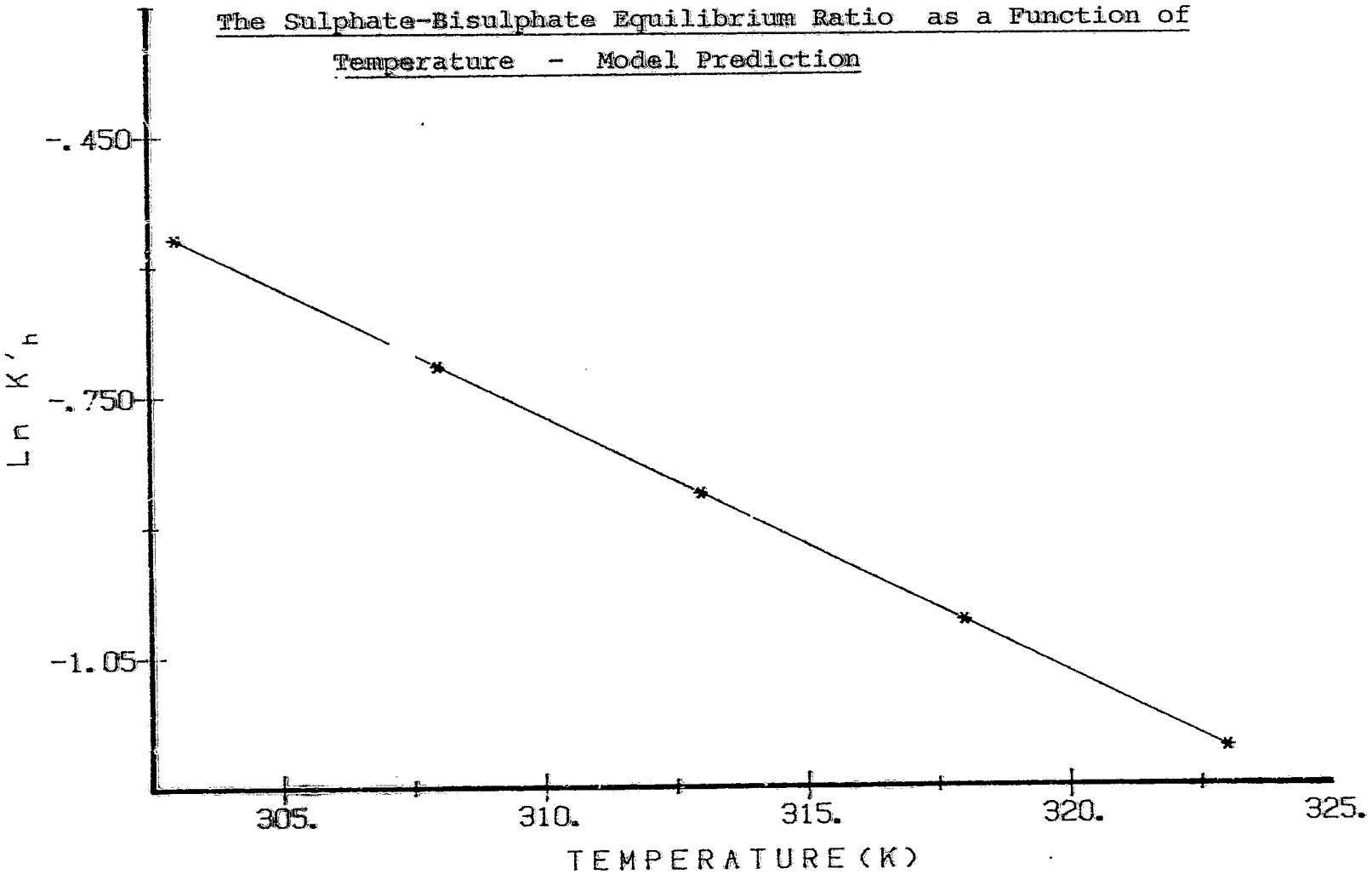
For the purpose of this dissertation,it was found that the equilibrium ratio

$$K_h' = \frac{Z_2 \, Z_6}{Z_7} = \exp\,(8{,}339 - 0{,}0294\ T) \qquad (2.9)$$

describes the situation to an accurate level.Figure 25 below shows this relationship in a graphic way.

FIGURE 25

The Sulphate-Bisulphate Equilibrium Ratio as a Function of Temperature - Model Prediction



APPENDIX E

Theory on Development of the Diaphragm Model

Transport of Ions in Solution(28)

Dilute Solution Theory

The flux of each ionic species may be expressed as

$$N_j = -z_j u_j F B_j \nabla V - D_j \nabla B_j + B_j v \qquad (E.1)$$

In this equation N_j represents the flux of species j and indicates the direction and rate of movement of the species. The three terms on the right side of the equation represent the three mechanisms of mass transfer:

(i) motion of a charged species in an electric field
(ii) molecular diffusion due to a concentration gradient
(iii) convection due to the bulk motion of the solution.

The current density of the solution can be expressed in terms of the fluxes of all the ions

$$i = F \sum_j z_j N_j \qquad (E.2)$$

The material balance for each species is

$$\frac{dB_i}{d\tau} = -\nabla N_j + r_j \qquad (E.3)$$

where r_j is the production rate of the jth species.Equations (E.2) and (E.3) are basic physical laws.All electrolytic solutions are electrically neutral in the bulk,except in a thin layer near the electrodes.Hence the following "accurate assumption" can be made

$$\sum_j z_j B_j = 0 \qquad \text{(E.4)}$$

In equation (E.1) an approximation has already been made as the driving force for the diffusion should be an activity gradient .Activities are equivalent to concentrations under dilute conditions , and concentrations are the ones considered in the referred equation.Another simplification made is that the bulk velocity was taken to be the velocity of all the species.Thus,when using the equation (E.1),one must be cautious due to its limitations.

Combining equatins (E.1) and (E.2) the following is the result

$$i = -F^2 \nabla V \sum_j z_j^2 u_j B_j - F \sum_j z_j D_j \nabla B_j + F v \sum_j z_j B_j \qquad \text{(E.5)}$$

From equation (E.4) the last term is zero,and in case of no concentration gradients then

$$i = K \nabla V \qquad \text{(E.6)}$$

where $K = F^2 \sum_j z_j^2 u_j B_j$ is the solution conductivity.

The fraction of current carried by species j, $t_j.i$, can be written in the case of no concentration variation as

$$t_j.i = -F^2 z_j^2 u_j B_j \nabla V = \frac{z_j^2 u_j B_j}{\sum_j z_j^2 u_j B_j}.i \qquad \text{(E.7)}$$

Hence

$$t_j = \frac{z_j^2 u_j B_j}{\sum_j z_j^2 u_j B_j} \qquad \text{(E.8)}$$

which is called the transport or transference number.

In a binary electrolyte(29) only two ions are present. Then

$$t_+ = \frac{z_+ u_+ B_+}{z_+^2 u_+ B_+ + z_-^2 u_- B_-} \qquad (E.9)$$

and

$$t_- = \frac{z_- u_- B_-}{z_+^2 u_+ B_+ + z_-^2 u_- B_-} \qquad (E.10)$$

If these equations are added then the following is concluded

$$t_+ + t_- = 1 \qquad (E.11)$$

The Nernst-Einstein equation provides a relationship between D_j, the diffusion coefficient, and u_j , the mobility of species j (28)

$$D_j = R\ T\ u_j \qquad (E.12)$$

Concentrated Solution Theory

Equation (E.1) should,for concentrated solutions,be replaced by

$$B_i \nabla \mu_i = \sum_j k_{ij}(v_j - v_i) = R\ T \sum_j \frac{B_i\ B_j}{B_T\ D_{ij}} \qquad (E.13)$$

where μ_i is the electrochemical potential of species i, k_{ij} is the friction coefficient that accounts for interactions between the various ions. D_{ij} is a "diffusion coefficient" allowing for interaction between species i and j, and v_j and v_i are the average velocities of species i and j(28).

As the ions present in the electrolytes,except for the hydrogen and hydroxide ions,have concentrations ranging from 0,2 to 3 Molar,the flux equation for dilute solutions should not be applied here.Therefore it is necessary to develop the concentrated solution flux equation.

If one considers the flux equation in only one direction perpendicular to the diaphragm plane,calling it the x-direction,then

$$B_i \frac{d\mu_i}{dx} = R\ T \sum_j \frac{B_i\ B_j}{B_T\ D_{ij}} (v_j - v_i) \qquad (E.14)$$

As the model is considered under steady-state assumption, the following conditions will hold

$$N_i = B_i\ v_i \qquad (E.15)$$

$$I = F \sum_j z_j\ N_j \qquad (E.16)$$

$$\frac{dN_i}{dx} = 0 \qquad (E.17)$$

$$\sum_j z_j\ B_j = 0 \qquad (E.18)$$

For convenience the electrochemical potential of an ion i, μ_i , is expressed as a sum of a chemical potential and an electrical potential as follows(30)

$$\mu_i = \mu_{io} + R\ T\ \ln \frac{B_i}{B_i^o} + z_i\ F(E-E^o) \qquad (E.19)$$

Then differentiating the above equation with respect to x and rearranging

$$\frac{B_i}{R\ T} \frac{d\mu_i}{dx} = \frac{dB_i}{dx} + \frac{B_i\ z_i\ F}{R\ T} \frac{dE}{dx} \qquad (E.20)$$

Assuming our system is a multicomponent one made up of water,manganese,ammonium and sulphate ions,having a total of n+1 and giving the subscript 0 for water, E.14 will become

$$B_i \frac{d\mu_i}{dx} = R\,T \sum_{j=0}^{n} \frac{B_i\,B_j}{B_T\,D_{ij}} (v_j - v_i) \qquad (E.21)$$

Extracting the first term from the summation one would obtain, after some rearrangement

$$v_i = v_o - \frac{D_{io}\,B_T}{B_o\,R\,T} \frac{d\mu_i}{dx} + \sum_{j=1}^{n} \frac{B_j\,D_{io}}{B_o\,D_{ij}} (v_j - v_i) \qquad (E.22)$$

Defining

$$D_i = \frac{B_{io}\,B_T}{B_o} \qquad (E.23)$$

and

$$K_i = \sum_{j=1}^{n} \frac{B_j\,D_{io}}{B_o\,D_{ij}} (v_j - v_i) \qquad (E.24)$$

Then equation (E.22) becomes

$$v_i = v_o - \frac{D_i}{R\,T} \frac{dV}{dx} + K_i \qquad (E.25)$$

Using (E.15), (E.20) and (E.25) on gets

$$N_i = B_i(v_o + K_i) - D_j \frac{dB_i}{dx} - \frac{B_i\,D_i\,z_i\,F}{R\,T} \frac{dV}{dx} \qquad (E.26)$$

Note that when $K_i = 0$, the equation reduces to the same form as for the dilute solution flux equation (E.5). Substituting (E.26) into (E.16) and using the electrical neutrality condition (E.18) one obtains

$$I = \sum_{j=1}^{n} z_j F B_j K_j - \sum_{j=1}^{n} z_j F D_j \frac{dB_j}{dx} - \frac{dV}{dx} \sum_{j=1}^{n} \frac{B_j D_j z_j^{\,2}\,F^2}{R\,T} \qquad (E.27)$$

Now it is required to eliminate the term $\frac{dV}{dx}$, as it is difficult to measure. That is done by solving for the electrical potential gradient term in (E.27) and substituting in equation (E.26) to obtain:

$$N_i = B_i(v_o + K_i) - \frac{t_i}{z_i} \sum_{j=1}^{n} z_j B_j K_j + \frac{I\, t_i}{z_i\, F} - D_i \frac{dB_i}{dx} +$$

$$+ \frac{t_i}{z_i} \sum_{j=1}^{n} z_j D_j \frac{dB_j}{dx} \qquad (E.28)$$

Bryson and Lawrence(18) further developed this condition, by finding that the following assumptions hold

$$-\frac{dV}{dx} \sum_{j=1}^{n} \frac{B_j\, D_j\, z_j^{\,2}\, F^2}{R\, T} \sum_{j=1}^{n} (z_j F B_j K_j - z_j F D_j \frac{dB_j}{dx}) \qquad (E.29)$$

Then equation (E.27) reduces to

$$I \simeq -\frac{dV}{dx} \frac{F^2}{R\, T} \sum_{j=1}^{n} B_j D_j z_j^{\,2} \qquad (E.30)$$

Furthermore, B_j can be replaced in (E.30) by the arithmetic mean concentration $B_j^{\,*}$ without introducing a significant error

$$B_j^{\,*} = \frac{1}{2}(Y_j + Z_j) \qquad (E.31)$$

Thus

$$\frac{F}{RT} \frac{dV}{dx} \simeq \frac{-I}{F \sum_{j=1}^{n} B_j^{\,*} D_j z_j^{\,2}} \qquad (E.32)$$

Substituting into equation(E.26) it leads to

$$N_i = B_i(u_0 + K_i) - D_i \frac{dB_i}{dx} + \frac{B_i D_i z_i I}{F \sum_{j=1}^{n} B_j^{\,*} D_j z_j^{\,2}} \qquad (E.33)$$

This equation multiplied by the area leads to the equation used in the model, (2.10)

$$AN_j = W_j = Q_c r_{j(x)} - \frac{I\ F\ D_j\ z_j\ B_j(x)}{R\ T\ K^*} - \varepsilon A\ D_j \frac{dB_j}{dx} \qquad (2.10)$$

APPENDIX F

Fitting the Kinetic Model

Equation(2.27) gives the kinetic model in the form

$$\xi_c = \frac{1}{1 + \frac{\lambda_2}{\lambda_1}\left[1 + \left(\frac{\lambda_4 - \lambda_2}{\lambda_2}\right)\frac{\lambda_3}{\lambda_1}\frac{Y_8}{Y_1}\right]\frac{Y_2}{Y_1}} \qquad (2.27)$$

Let

$$\eta = 1 + \left(\frac{\lambda_4 - \lambda_2}{\lambda_2}\right)\frac{\lambda_3}{\lambda_1}\frac{Y_8}{Y_1} = A + B\frac{Y_8}{Y_1} \qquad (F.1)$$

and solving for $\frac{\lambda_2}{\lambda_1}$ we will obtain

$$\frac{\lambda_2}{\lambda_1} = \frac{1}{\eta}\frac{(1 - \xi_c)}{\xi_c}\frac{Y_1}{Y_2} \qquad (F.2)$$

This equation is of the form used to obtain the fitting of the Delta Manganese data,as well as the MINTEK's.

Fitting the Impurity Level

From the sets of data the constants A and B from the kinetic model expression (2.27) incorporating the impurity level were fitted as well as possible.The equation has a linear form

$$\eta = A + B\frac{Y_8}{Y_1} \qquad (F.1)$$

The values for the constants used in the model are

$$A = 0{,}72919681 \qquad (F.3)$$
$$B = 1{,}3479702 \times 10^3$$

Figure 26 shows the plot of η versus Y_8/Y_1 ,from which the constants resulted.The following are worth noting:

(i) the readings are very spread,giving a large variance

(ii) the impurities were expressed as a total impurity level,as there was not enough data to study the effects of the individual impurities

(iii) as the expected trend was linear it was decided to fit the best straight line through the points, thus explaining the operational data.

Fitting the Current Density Effect

From the MINTEK data(6) it can be found that the relationship between the cathodic current efficiency and current density is quadratic,going through a maximum.By plotting the results tabulated in Table 26 yields Figure 27,in which the MINTEK results are compared to the model predictions. Please note that here no correction factor had been taken into account due to the fact that the operational data from Delta was consistently higher than that of MINTEK, when considering the fractional current efficiency.The way the equation was rearranged to fit the MINTEK data is shown on Figure 27.

It can be observed that in the area around the optimum, the fitted model agrees with the experimental readings within 5%.Only at very low current densities the error involved is in the order of 10%.

The model used has the following form,which was obtained from equation (F.2)

$$\left[\frac{(1 - \xi_c)}{\xi_c}\right] = 49,78009(i-550)^2 - 472,4760(i-550) + 3,8947157 \times 10^6 \qquad (F.4)$$

FIGURE 26 - Fitting the Impurity Model

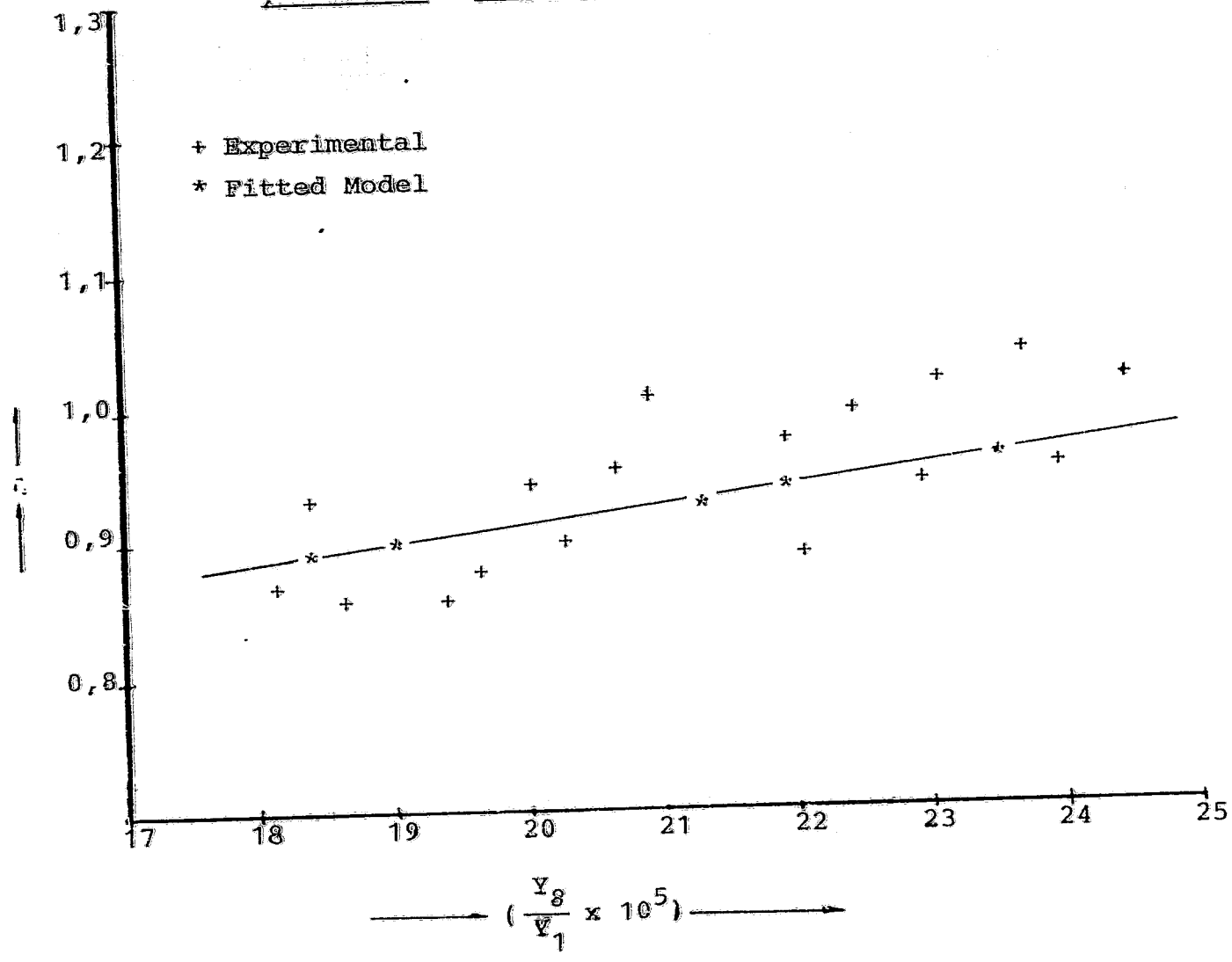


FIGURE 26 - Fitting the Impurity Model

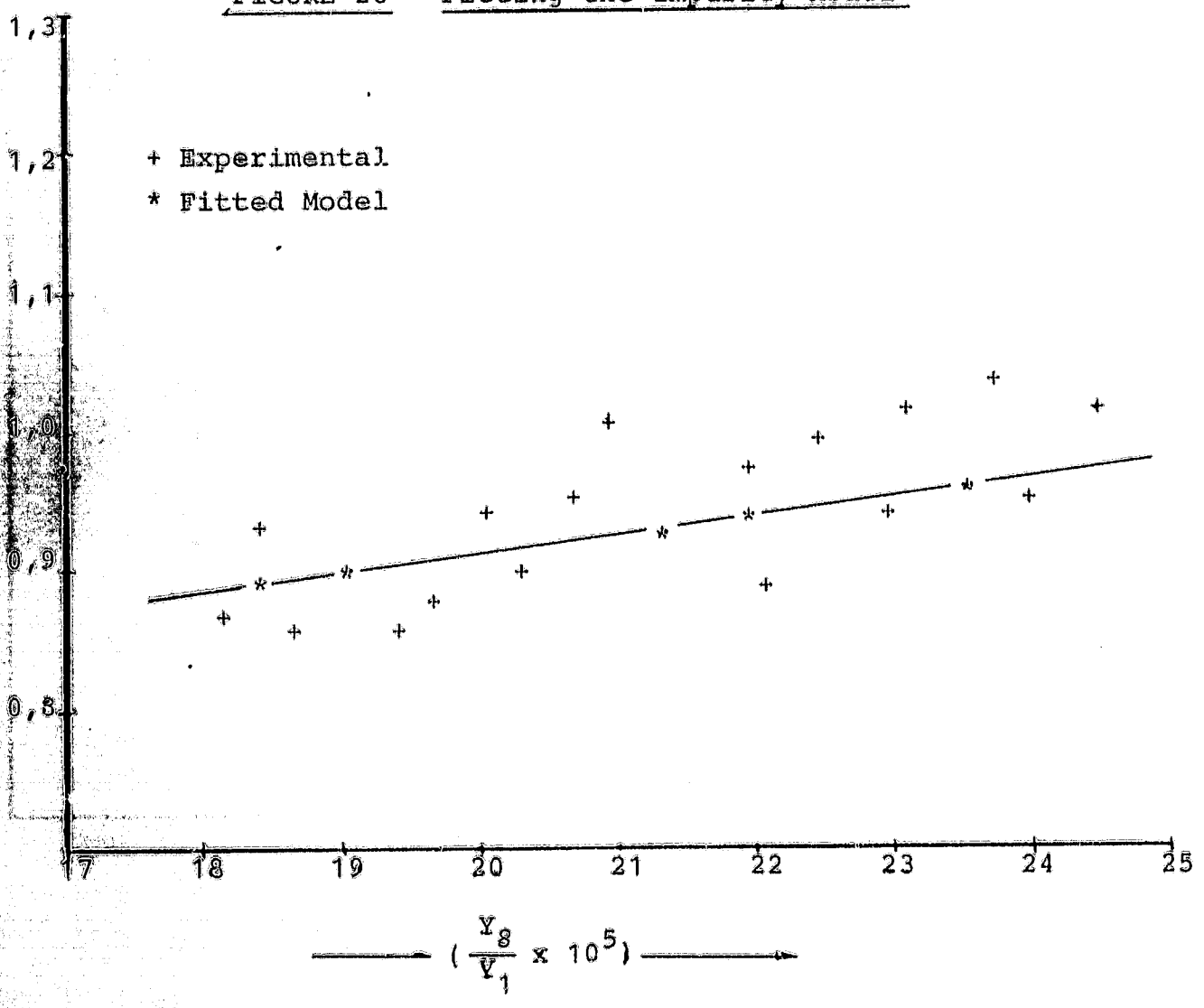


FIGURE 27 FITTING CURRENT DENSITY EFFECT

$$Y = \frac{(1 - \varepsilon_c)}{\varepsilon_c} \frac{Y_1}{Y_2}$$

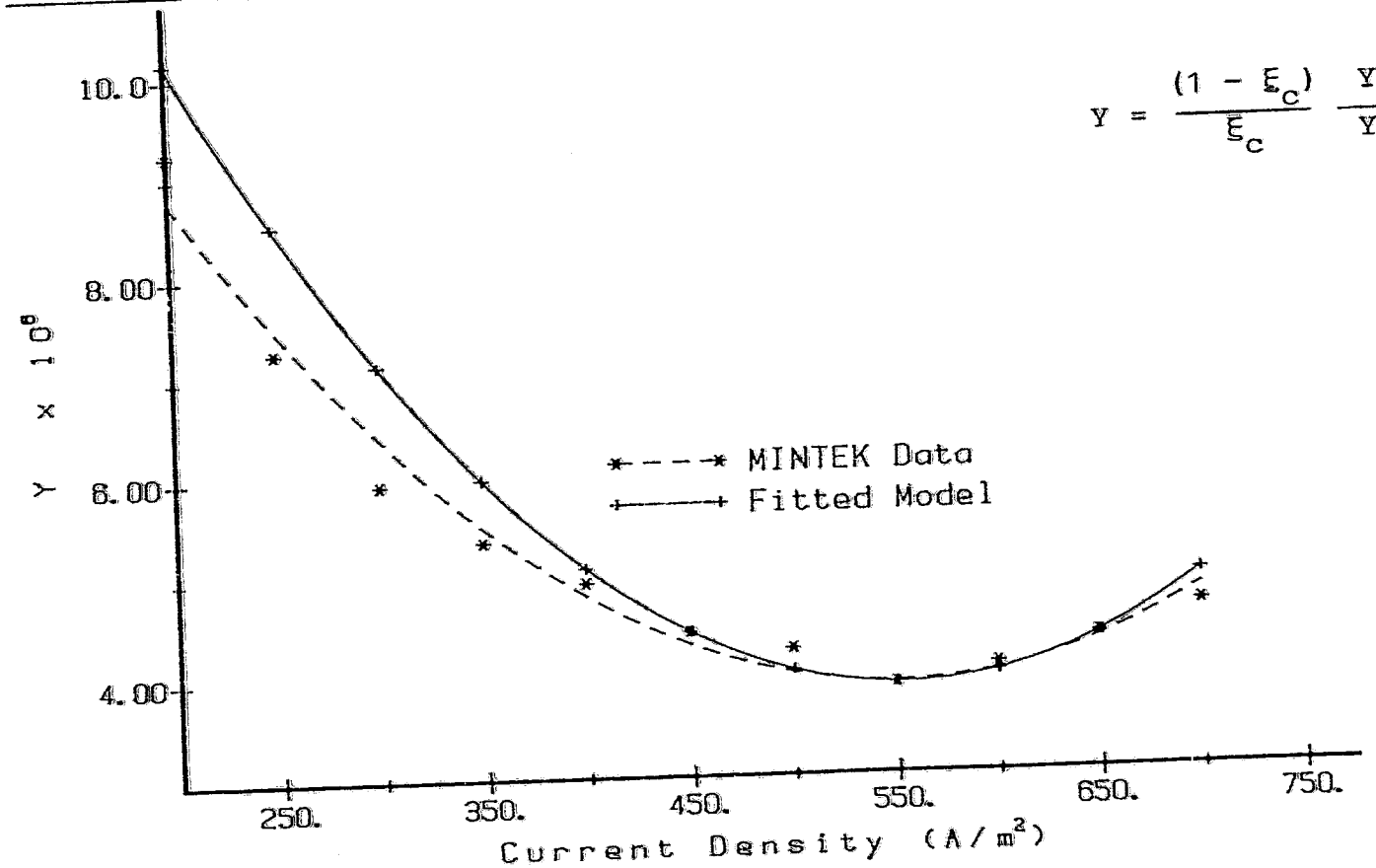


TABLE 26 - Fitting the Current Density Effect on the Kinetic Model

i (A/m²)	MINTEK $Y=\frac{(1-\xi_c)}{\xi_c}\frac{Y_1}{Y_2}$	MODEL $Y=\frac{(1-\xi_c)}{\xi_c}\frac{Y_1}{Y_2}$	% Error
200	$9,2393663\times10^{6}$	$10,158143\times10^{6}$	9,04
250	$7,2632819\times10^{6}$	$8,516666\times10^{6}$	14,71
300	$5,939526\times10^{6}$	$7,1240903\times10^{6}$	16,63
350	$5,3627937\times10^{6}$	$5,9804145\times10^{6}$	10,30
400	$4,9356752\times10^{6}$	$5,0856391\times10^{6}$	2,95
450	$4,4397642\times10^{6}$	$4,4397647\times10^{6}$	0,00
500	$4,252856\times10^{6}$	$4,0422789\times10^{6}$	5,00
550	$3,8947157\times10^{6}$	$3,8947157\times10^{6}$	0,00
600	$4,0708548\times10^{6}$	$3,8955421\times10^{6}$	1,88
650	$4,3452690\times10^{6}$	$4,3452690\times10^{6}$	0,00
700	$4,6332906\times10^{6}$	$4,9438963\times10^{6}$	6,65

Fitting the Temperature Effect

The expected trend for the temperature is of the exponential type. The model was found to be

$$\frac{(1-\xi_c)}{\xi_c}\frac{Y_1}{Y_2} = A\exp\left(\frac{B}{T}\right) + C \qquad (F.5)$$

where

$A = 4,2589946 \times 10^{-12}$

$B = 12,587794 \times 10^{4}$

$C = 2,6000000 \times 10^{6}$

These values were found by fitting a straight line to the logarithmic plot as shown in Figure 28. The best straight

line was fitted to the MINTEK (6) results and then the model has been run at the same conditions and compared to the results.These are tabulated in Table 27 and plotted in Figure 28.The results agree within 2,5%.

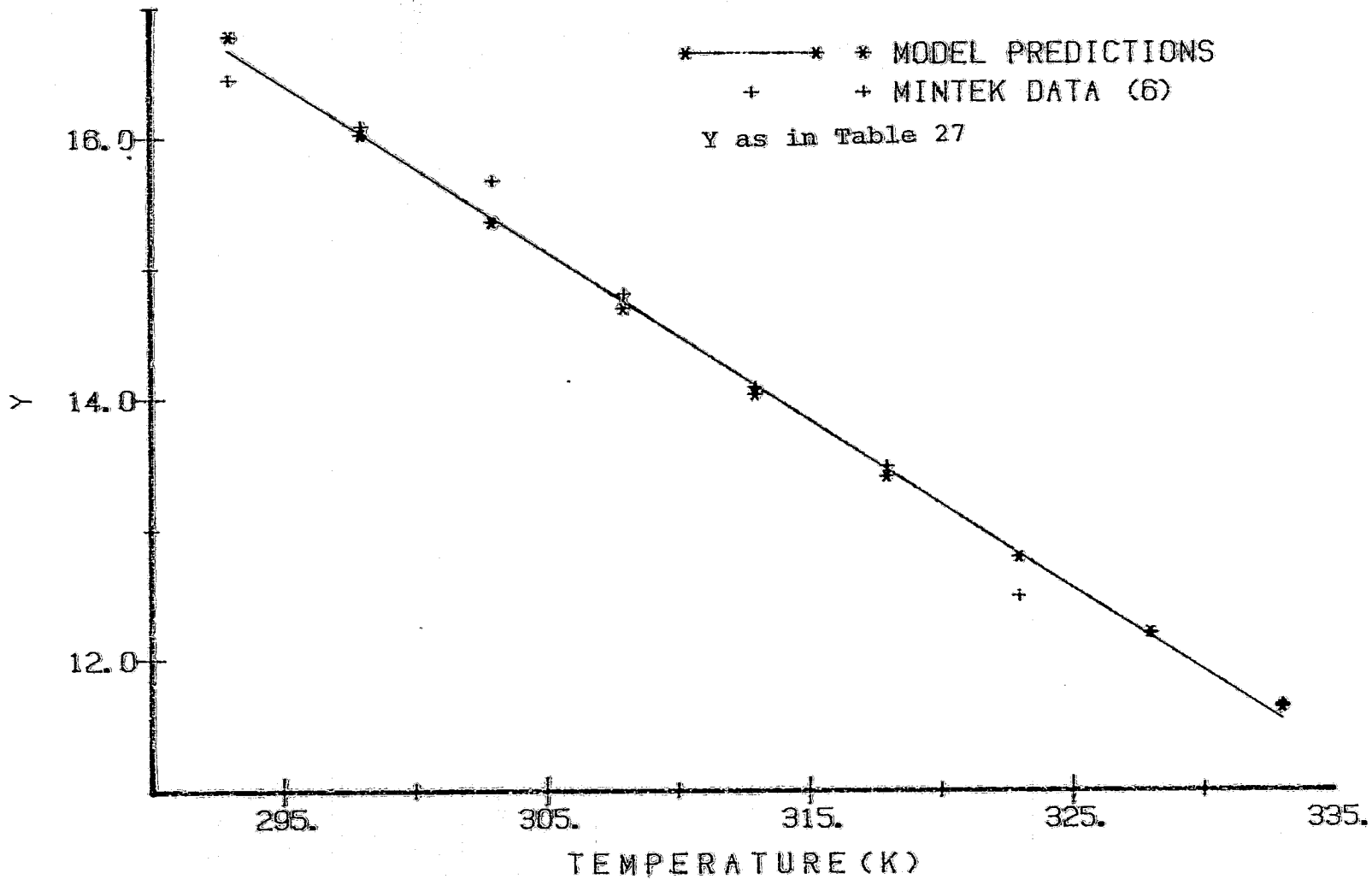
TABLE 27 - Fitting the Temperature Effect

All results at 550A/m²

t (°C)	MINTEK $Y=\ln\left[\left(\frac{1-\xi_c}{\xi_c}\frac{Y_1}{Y_2}\right)-2{,}6\times10^6\right]$	MODEL Y	%Error
20	16,448937	16,780153	2,01
25	16,089197	16,024885	0,40
30	15,671057	15,[illegible]732	2,00
35	14,803890	14,690579	0,77
40	14,088244	14,036014	0,37
45	13,482339	13,406624	0,56
50	12,487183	12,789822	2,36
55	12,193645	12,198196	0,03
60	11,638676	11,619157	0,16

By joining (F.3),(F.4) and (F.5) together,the general effect of λ_2/λ_1 was derived and the form used in the computer model is as in equation (2.32) with the value of γ as $1{,}36\times10^6$ (equation 2.33).

FIGURE 28 FITTING THE TEMPERATURE EFFECT



APPENDIX G

Modelling the Water Losses

Equation(2.53) was derived from the data in the Steam Tables (23)to estimate the mole fraction of water vapour versus temperature.The follcwing equation was found to give the best fitting in the range $310 < T < 320$

$$y_o = z_o = -1,267 + 0,00428\ T \qquad (2.53)$$

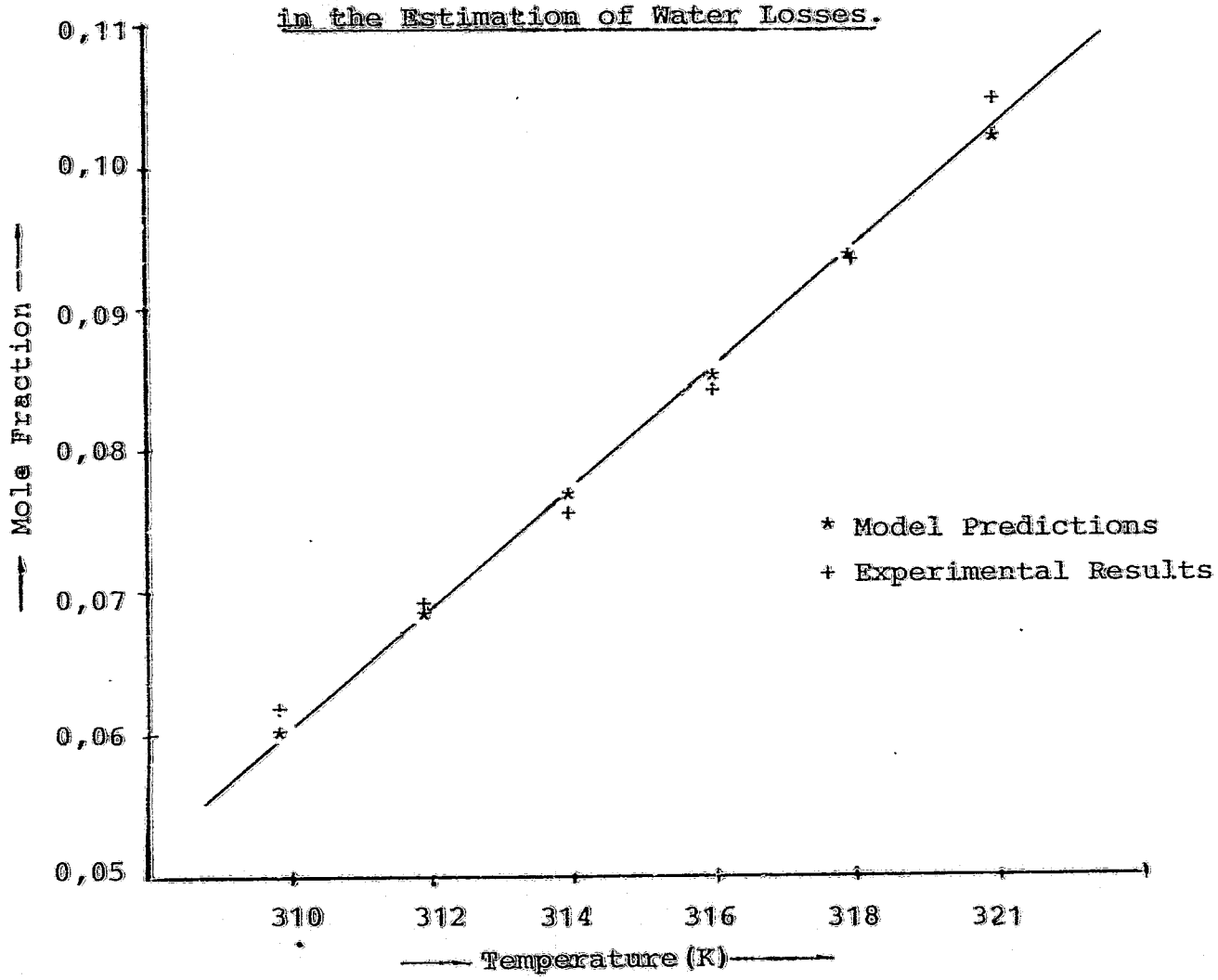
The comparison between model predictions and experimental data are presente both in Table 28 and Figure 29.

TABLE 28 - Fitting the Mole Fraction Equation from Steam Tables(23)

T (°C)	T (K)	Experimental Partial Pressure (bar)	Experimental Mole Fraction	Model Mole Fraction
37	310	0,0628	0,06198	0,05980
38	311	0,06624	0,06537	0,06408
39	312	0,0700	0,06908	0,06836
40	313	0,07375	0,07279	0,07264
41	314	0,07787	0,07685	0,07692
42	315	0,08198	0,08091	0,08120
43	316	0,08649	0,08536	0,08548
44	317	0,09100	0,08981	0,08976
45	318	0,09595	0,09470	0,09404
46	319	0,10090	0,09958	0,09832
47	320	0,10625	0,10486	0,10260

$$\text{mole fraction} = \frac{p}{p_{atm}} = \frac{p\,(\text{bar})}{1,01325\,(\text{bar})}$$

FIGURE 29 - Comparison Between Experimental Results and Model Predictions for the Mole Fraction versus Temperature in the Estimation of Water Losses.



Author Rodrigues J C P
Name of thesis Modelling the performance of Manganese Eletrowinning cells 1983

PUBLISHER:
University of the Witwatersrand, Johannesburg
©2013

LEGAL NOTICES:

Copyright Notice: All materials on the University of the Witwatersrand, Johannesburg Library website are protected by South African copyright law and may not be distributed, transmitted, displayed, or otherwise published in any format, without the prior written permission of the copyright owner.

Disclaimer and Terms of Use: Provided that you maintain all copyright and other notices contained therein, you may download material (one machine readable copy and one print copy per page) for your personal and/or educational non-commercial use only.

The University of the Witwatersrand, Johannesburg, is not responsible for any errors or omissions and excludes any and all liability for any errors in or omissions from the information on the Library website.

Author Rodrigues J C P
Name of thesis Modelling the performance of Manganese Eletrowinning cells 1983

PUBLISHER:
University of the Witwatersrand, Johannesburg
©2013

LEGAL NOTICES:

Copyright Notice: All materials on the University of the Witwatersrand, Johannesburg Library website are protected by South African copyright law and may not be distributed, transmitted, displayed, or otherwise published in any format, without the prior written permission of the copyright owner.

Disclaimer and Terms of Use: Provided that you maintain all copyright and other notices contained therein, you may download material (one machine readable copy and one print copy per page) for your personal and/or educational non-commercial use only.

The University of the Witwatersrand, Johannesburg, is not responsible for any errors or omissions and excludes any and all liability for any errors in or omissions from the information on the Library website.